THE JOURNAL OF BIOLOGICAL CHEMISTRY VOL. 289, NO. 20, pp. 14194–14210, May 16, 2014

Group VIA Phospholipase A_2 Mitigates Palmitate-induced β-Cell Mitochondrial Injury and Apoptosis*[S]

Received for publication, February 27, 2014, and in revised form, March 17, 2014 Published, JBC Papers in Press, March 19, 2014, DOI 10.1074/jbc.M114.561910

Haowei Song[‡], **Mary Wohltmann**[‡], **Min Tan**[‡], **Jack H. Ladenson**[§], **and John Turk**[‡1]

From the [‡]*Mass Spectrometry Resource, Division of Endocrinology, Metabolism, and Lipid Research, Department of Medicine and* [§]*Division of Laboratory and Genomic Medicine, Department of Pathology and Immunology, Washington University School of Medicine, St. Louis, Missouri 63110*

Background: Lipid-induced β-cell loss contributes to type 2 diabetes mellitus (T2DM).
Results: Palmitate-induced β-cell lipid oxidation, mitochondrial dysfunction, and apoptosis correlate inversely with expression of iPLA$_2$β, which associates with mitochondria, generates monolysocardiolipin, and lowers oxidized phospholipid content.
Conclusion: iPLA$_2$β mitigates palmitate-induced β-cell mitochondrial injury and apoptosis and may facilitate repair of oxidized lipids.
Significance: Understanding lipid-induced β-cell loss could lead to T2DM therapies.

Palmitate (C16:0) induces apoptosis of insulin-secreting β-cells by processes that involve generation of reactive oxygen species, and chronically elevated blood long chain free fatty acid levels are thought to contribute to β-cell lipotoxicity and the development of diabetes mellitus. Group VIA phospholipase A_2 (iPLA$_2$β) affects β-cell sensitivity to apoptosis, and here we examined iPLA$_2$β effects on events that occur in β-cells incubated with C16:0. Such events in INS-1 insulinoma cells were found to include activation of caspase-3, expression of stress response genes (C/EBP homologous protein and activating transcription factor 4), accumulation of ceramide, loss of mitochondrial membrane potential, and apoptosis. All of these responses were blunted in INS-1 cells that overexpress iPLA$_2$β, which has been proposed to facilitate repair of oxidized mitochondrial phospholipids, *e.g.* cardiolipin (CL), by excising oxidized polyunsaturated fatty acid residues, *e.g.* linoleate (C18:2), to yield lysophospholipids, *e.g.* monolysocardiolipin (MLCL), that can be reacylated to regenerate the native phospholipid structures. Here the MLCL content of mouse pancreatic islets was found to rise with increasing iPLA$_2$β expression, and recombinant iPLA$_2$β hydrolyzed CL to MLCL and released oxygenated C18:2 residues from oxidized CL in preference to native C18:2. C16:0 induced accumulation of oxidized CL species and of the oxidized phospholipid (C18:0/hydroxyeicosatetraenoic acid)-glycerophosphoethanolamine, and these effects were blunted in INS-1 cells that overexpress iPLA$_2$β, consistent with iPLA$_2$β-mediated removal of oxidized phospholipids. C16:0 also induced iPLA$_2$β association with INS-1 cell mitochondria, consistent with a role in mitochondrial repair. These findings indicate that iPLA$_2$β confers significant protection of β-cells against C16:0-induced injury.

Chronic elevation of free fatty acids (FFAs)[2] in blood and tissues, alone or combined with hyperglycemia, is associated with both insulin resistance and type 2 diabetes mellitus (1–3). Results from several laboratories suggest that islet accumulation of lipid is deleterious and eventuates in β-cell failure and death in a process designated "lipotoxicity," and FFAs have been shown to cause β-cell death by both apoptosis and necrosis (4–7). Although the molecular and cellular mechanisms underlying FFA-induced β-cell apoptosis are not fully understood, participating processes include generation of reactive oxygen species (ROS) and mitochondrial dysfunction (8–11), production of ceramide and nitric oxide (NO) (4, 12), and induction of endoplasmic reticulum stress (13–18).

The lipid-metabolizing enzyme Group VIA phospholipase A_2 (iPLA$_2$β) plays signaling roles in insulin secretion, promotes β-cell proliferation, and affects responses to stimuli that induce apoptosis (19–23). Here we examined palmitate-induced apoptosis of INS-1 insulinoma cells and of native pancreatic islet β-cells and found that β-cells with increased or reduced iPLA$_2$β activity have blunted or enhanced sensitivity, respectively, to palmitate-induced injury. The reduction in palmitate-induced apoptosis of INS-1 cells that overexpress iPLA$_2$β is associated with attenuation of the effects of palmitate to activate capase-3 and to cause collapse of the mitochondrial membrane potential ($\Delta\Psi_m$). Incubation of β-cells with palmitate was found to result in subcellular redistribution of iPLA$_2$β and its association with mitochondria where it appears to participate in remodeling oxidized phospholipid species, including cardiolipin.

* This work was supported, in whole or in part, by National Institutes of Health Grants R37-DK34388, P41-RR00954, P60-DK20579, and P30-DK56341.

[S] This article contains supplemental Figs. S1–S3.

[1] To whom correspondence should be addressed: Washington University School of Medicine, Campus Box 8127, 660 S. Euclid Ave., St. Louis, MO 63110. Tel.: 314-362-2602; Fax: 314-362-7641; E-mail: jturk@dom.wustl.edu.

[2] The abbreviations used are: FFA, free fatty acid; ATF4, activating transcription factor 4; C16:0, palmitate; C18:2, linoleate; CHOP, C/EBP (CCAAT/enhancer-binding protein) homologous protein; CL, cardiolipin; DNPH, dinitrophenylhydrazine; GPE, glycerophosphoethanolamine; iPLA$_2$β, Group VIA phospholipase A_2; iPLA$_2$γ, Group VIB PLA$_2$; 4-HNE, 4-hydroxynonenal; HETE, hydroxyeicosatetraenoic acid; iNOS, inducible nitric-oxide synthase; MLCL, monolysocardiolipin; MS/MS, tandem mass spectrometry; OE, overexpressing; PLA$_2$, phospholipase A_2; ROS, reactive oxygen species; TG, transgenic; $\Delta\Psi_m$, mitochondrial membrane potential; COX IV, cytochrome *c* oxidase complex IV; ESI, electrospray ionization; PUFA, polyunsaturated fatty acid; oxy, oxidized.

EXPERIMENTAL PROCEDURES

Materials—Most materials were obtained from sources specified previously (21–24). Rainbow molecular mass standards, PVDF membranes, and Triton X-100 were obtained from Bio-Rad. SuperSignal West Femto Substrate was from Thermo Fisher. Coomassie reagent and SDS-PAGE supplies were from Invitrogen. Palmitate, dinitrophenylhydrazine (DNPH), collagenase, protease inhibitor mixture, common reagents, and salts were from Sigma. Bovine serum albumin (BSA; fatty acid-free, fraction V) was from MP Biomedicals (Solon, OH). Synthetic phospholipids were from Avanti Polar Lipids (Alabaster, AL). 4-Hydroxynonenal (4-HNE) and d_3-4-HNE were from Cayman Chemicals (Ann Arbor, MI). Solvents were from Fisher Scientific.

Generation of Genetically Modified Mice and Wild-type Littermates—All animal protocols were approved by the Washington University Animal Studies Committee. Preparation and characterization of global iPLA$_2\beta$ knock-out (KO) mice (25, 26), transgenic (TG) mice that overexpress iPLA$_2\beta$ in pancreatic islet β-cells (27), and their wild-type littermates on a C57BL/6 genetic background have been described previously as have genotyping procedures for these mice (25–27).

Islet Isolation—Islets were isolated from minced pancreata of male mice by collagenase digestion followed by Ficoll step density gradient separation and stereomicroscopic manual selection to exclude contaminating tissues as described (26–28). Mouse islets were counted, and aliquots of homogenate were used for Coomassie protein determinations and other measurements.

Cell Culture—Preparation and properties of stably transfected iPLA$_2\beta$-OE INS-1 rat insulinoma cells that overexpress iPLA$_2\beta$, control INS-1 cells stably transfected with empty vector only, and iPLA$_2\beta$ knockdown INS-1 cells in which iPLA$_2\beta$ expression is knocked down by siRNA have been described previously (24, 29, 30). INS-1 cell lines were cultured as described (24) in RPMI 1640 medium containing 11 mM glucose, 10% fetal calf serum, 10 mM HEPES buffer, 2 mM glutamine, 1 mM sodium pyruvate, 50 mM β-mercaptoethanol, 100 units/ml penicillin, and 100 μg/ml streptomycin. Medium was replaced with fresh medium every 2 days, and cell cultures were divided once weekly. Cells were grown to 80% confluence and harvested after treatment described in the figure legends. All incubations were performed at 37 °C under 95% air, 5% CO_2.

Immunoblotting Analyses—Cells were harvested and sonicated (15–30 s at 1-s intervals) in appropriate buffer, and an aliquot (30 μg) of lysate protein was analyzed by SDS-PAGE (4–20% Tris-glycine gel, Invitrogen), transferred onto Immobilon-P polyvinylidene difluoride membranes (Bio-Rad), and processed for immunoblotting analyses as described (21–24). Targeted proteins and primary antibody concentrations were as follows: iPLA$_2\beta$ (1:2000 dilution of T-14 antibody from Santa Cruz Biotechnology, Santa Cruz, CA, sc-14463), caspase-3 (1:1000 dilution of H-277 antibody from Santa Cruz Biotechnology, sc7148), cytochrome *c* oxidase complex IV (COX IV) (1:1000 dilution of antibody 4844 from Cell Signaling Technology, Beverly, MA), anti-FLAG (1:1000; Sigma, F1804), and anti-polyhistidine (1:1000; Sigma, H1029). Secondary antibody concentration was 1:10,000. Immunoreactive bands were visualized by enhanced chemiluminescence (ECL).

Caspase-3 Activation—Caspase-3 activation was measured as described (19, 20, 22) in INS-1 cells after incubation with palmitate or vehicle by homogenizing the cells and analyzing extracted protein electrophoretically on a 4–20% Tris-glycine gel (Invitrogen, EC6028PK5). The activated 17-kDa isoform (p17) was detected with antibody against caspase-3 (H-277) (Santa Cruz Biotechnology). A luminescence-based assay was performed (31) with a commercial kit (G8090, Promega, Madison, WI) for isolated islets according to the manufacturer's instructions.

Quantitative Real Time PCR—As described (26, 27, 30), total RNA was extracted from INS-1 cells using a Qiagen RNeasy Mini kit (catalog number 74104), and aliquots from samples for each condition were prepared that contained equal amounts of RNA. SuperScript III (Invitrogen, catalog number 18080-044) enzyme was used to generate cDNA from the RNA template. PCR amplification mixtures (25 μl) contained SYBR Green PCR Master Mix (12.5 μl, 2×, Applied Biosystems, catalog number 4309155), a mixture (1.5 μl) of reverse and forward primers (30 nM), water (9 μl), and cDNA template (2 μl). Real time quantitative PCR was performed using the GeneAmp 5700 Sequence Detection System (PerkinElmer Life Sciences) with the following cycling parameters: polymerase activation (10 min at 95 °C) and amplification (40 cycles of 15 s at 95 °C and then 1 min at 60 °C). Relative expression levels were normalized to the endogenous control 18 S rRNA. Primer sets used were: 1) C/EBP homologous protein (CHOP) (forward, 5′-CTC ATC CCC AGG AAA CGA AG-3′; reverse, 5′-GAA CTC TGA CTG GAA TCT GGA G-3′); 2) activating transcription factor 4 (ATF4) (forward, 5′-CCA AGC ACT TCA AAC CTC ATG-3′; reverse, 5′-GTC CAT TTT CTC CAA CAT CCA ATC-3′), and 3) inducible nitric-oxide synthase (iNOS) (forward, 5′-CGT-GTG CCT GCT GCC TIC CTG CTG T-3′; reverse, 5′-GTA ATC CTCAAC CTG CTC CTC ACT C-3′).

Lipid Extraction—As described (24, 26), islets or INS-1 cells were placed in a solution (2 ml) of chloroform/methanol (1:1, v/v), homogenized, and sonicated on ice (20% power, 5-s bursts for 60 s; Vibra Cell probe sonicator; Sonics and Materials, Danbury, CT). After centrifugation (2,800 × *g*, 5 min) to remove tissue debris, supernatants were transferred to silanized 10-ml glass tubes and extracted with methanol (1 ml), chloroform (1 ml), and water (1.8 ml). Samples were Vortex-mixed and centrifuged (900 × *g*, 5 min). Supernatants were removed, concentrated, and dissolved in methanol/chloroform (9:1), and lipid phosphorus content was determined.

Ceramide Analyses by Electrospray Ionization Tandem Mass Spectrometry (ESI/MS/MS)—INS-1 cells were collected by centrifugation, and extraction buffer (chloroform/methanol/LiCl (20 mM), 2/2/1.8, v/v/v) was added to the cell pellet along with C8:0-ceramide ($[M + Li]^+$ m/z 432) internal standard (500 ng) as described (32). After Vortex-mixing and centrifugation (800 × *g*), the organic (lower) phase was collected, concentrated to dryness under nitrogen, and reconstituted in chloroform/methanol (1:1, v/v) containing 0.6% LiCl. Abundances of individual ceramide molecular species relative to the C8:0-ceramide internal standard were measured on a ThermoElectron

(San Jose, CA) Vantage triple quadruple mass spectrometer by ESI/MS/MS scanning for constant neutral loss of 48, which reflects elimination of formaldehyde and water from $[M + Li]^+$ (21, 32).

Detection of Apoptosis by Annexin V-FLUOS Staining—INS-1 cell apoptosis was determined as described (20, 22, 23) by measuring phosphatidylserine externalization in early apoptosis using an Annexin V-FLUOS staining kit (Roche Applied Science) to stain cells with fluorescein isothiocyanate-conjugated Annexin V according to the manufacturer's protocol in medium that also contained propidium iodide, which stains late stage apoptotic and necrotic cells. Briefly, about 10^6 cells were harvested, washed with PBS by centrifugation ($200 \times g$, 5 min), and resuspended in Annexin-V-FLUOS labeling solution (100 μl). Cells were incubated (15 min, 20 °C) and then analyzed by flow cytometry on a BD FACSCalibur (BD Biosciences) instrument at an excitation wavelength of 488 nm, and data were processed with WinMDI 2.9 software. Cells in early stage apoptosis were annexin V-positive and propidium iodide-negative, and those in late stage apoptosis were both annexin V- and propidium iodide-positive.

Assessment of Mitochondrial Membrane Potential by Flow Cytometry—Loss of $\Delta\Psi_m$ was measured as described (19, 20) in INS-1 cells with a commercial kit according to the manufacturer's instructions (Cell Technology, Inc.). Briefly, cells were washed twice with phosphate-buffered saline, resuspended in JC-1 reagent solution (0.5 ml), incubated (37 °C, 15 min), washed twice with PBS (1 ml), reconstituted in assay buffer (0.5 ml), and transferred to fluorescence-activated cell sorting tubes. Cellular fluorescence was analyzed with a BD FACSCalibur (BD Biosciences) flow cytometer in the FL2 channel.

Subcellular Fractionation to Isolate Mitochondria and Determine iPLA$_2\beta$ Association—INS-1 cell mitochondria were separated from cytosol as described (22) with minor modifications. Briefly, isolation buffer (5 volumes; 20 mM HEPES-KOH, 100 mM KCl, 1.5 mM $MgCl_2$, 1 mM EGTA, 250 mM sucrose) plus the protease inhibitor phenylmethylsulfonyl fluoride (1 mM) and protease inhibitor mixture (50 μl/ml) were added to the cell pellet (20 min, on ice). Cells were then homogenized (Dounce apparatus, 20 strokes), and the homogenate was centrifuged ($750 \times g$, 5 min). The pellet containing any remaining intact cells and nuclei was discarded. Supernatant was centrifuged ($10^5 \times g$, 15 min) to remove mitochondria (pellet), and that supernatant was ultracentrifuged ($10^6 \times g$, 1 h). Alternatively, mitochondrial and cytosolic fractions were isolated from cells with a Mitochondria/Cytosol Fractionation kit (BioVsion Research Products) and centrifugation as described (19). Isolated mitochondria were sonicated (200 μl of PBS, on ice), and aliquots of mitochondrial and cytosolic proteins were analyzed by SDS-PAGE and immunoblotted with antibodies to iPLA$_2\beta$ (T-14, Santa Cruz Biotechnology) and the mitochondrial marker COX IV subunit II (Molecular Probes, Eugene, OR). Densitometric ratios of bands from immunoblots were determined with AlphaEaseFC software.

Phospholipase A_2 Enzymatic Activity—Ca^{2+}-independent PLA_2 enzymatic activity was assayed as described (33) by ethanolic injection of substrate (1-palmitoyl-2-[^{14}C]linoleoyl-*sn*-glycero-3-phosphocholine) into assay buffer (40 mM Tris (pH 7.5), 5 mM EGTA) and monitoring release of [^{14}C]linoleate by TLC.

Immunostaining and Fluorescence Microscopic Analyses—As described (34, 35), stably transfected INS-1 cells that expressed an iPLA$_2\beta$-GFP construct were cultured on glass coverslips (18-mm diameter) in 6-well plates. After treatment, cells were stained with MitoTracker Red (Invitrogen, M7512) according to the manufacturer's protocol. Coverslips were then removed from the plate and sealed with a drop of ProLong Gold antifade reagent on glass slides that were examined with a Nikon TE300 microscope.

In Situ Detection of DNA Cleavage by TUNEL and DAPI Staining—TUNEL assays were performed essentially as described (21, 36). In brief, after treatment, INS-1 cells were washed twice with ice-cold PBS, immobilized on slides by cytospin, fixed (4% paraformaldehyde in PBS (pH 7.4) (1 h, room temperature), washed with PBS, and incubated in permeabilization solution (0.1% Triton-X-100 in 0.1% sodium citrate, PBS; 30 min, room temperature). That solution was then removed, TUNEL reaction mixture (50 μl) was added, and cells were incubated (1 h, 37 °C) in a humidified chamber, washed again with PBS, and counterstained with DAPI (1 μg/ml in PBS, 10 min) to identify nuclei. The incidence of apoptosis was assessed under a fluorescence microscope (Nikon Eclipse TE300) using a fluorescein isothiocyanate filter. Cells with TUNEL-positive nuclei were considered apoptotic. DAPI staining was used to determine the total number of cells in a field.

Preparation of Recombinant Group VIA PLA$_2$ with an N-terminal Polyhistidine Tag and a C-terminal FLAG Tag—Recombinant lentivirus containing cDNA encoding rat pancreatic islet iPLA$_2\beta$ with an N-terminal polyhistidine tag and a C-terminal FLAG tag were prepared, and the recombinant virus was used to achieve stable transfection of INS-1 cells that expressed the fusion protein as described (37). Recombinant His-iPLA$_2\beta$-FLAG was purified by immobilized metal affinity chromatography on cobalt-based TALON columns as described (34, 38).

Measurement of ROS Production by INS-1 Insulinoma Cells—Intracellular ROS production was measured with an OxiSelect^{TM} Intracellular ROS Assay kit according to the manufacturer's instructions (Cell Biolabs, Inc., San Diego, CA). The assay principle is that ROS oxidize 2′,7′-dichlorodihydrofluorescin to fluorescent 2′,7′-dichlorofluorescein. Fluorescence is then measured with a plate reader using excitation and emission wavelengths of 480 and 530 nm, respectively, and quantitation is performed relative to an eight-point 2′,7′-dichlorofluorescein standard curve (0–10,000 nM).

HPLC/ESI/MS/MS Analysis of 4-HNE from INS-1 Cells—Analysis of 4-HNE was performed essentially as described (39). Briefly, extracted INS-1 cell phospholipids were mixed with d_3-4-HNE internal standard and concentrated to dryness under N_2. Saturated DNPH solution (0.5 ml) containing 1 N HCl was added to the residue and incubated in the dark (2 h, room temperature). DNPH derivatives were extracted twice with CH_2Cl_2 and concentrated to dryness under N_2. Samples were reconstituted with isopropanol/acetonitrile/water (65:50:5, v/v/v) and analyzed by LC/ESI/MS/MS on a Thermo Finnegan TSQ Quantum Vantage mass spectrometer equipped with a Finnigan Surveyor Plus pump. Reverse-phase HPLC was performed on a Sigma

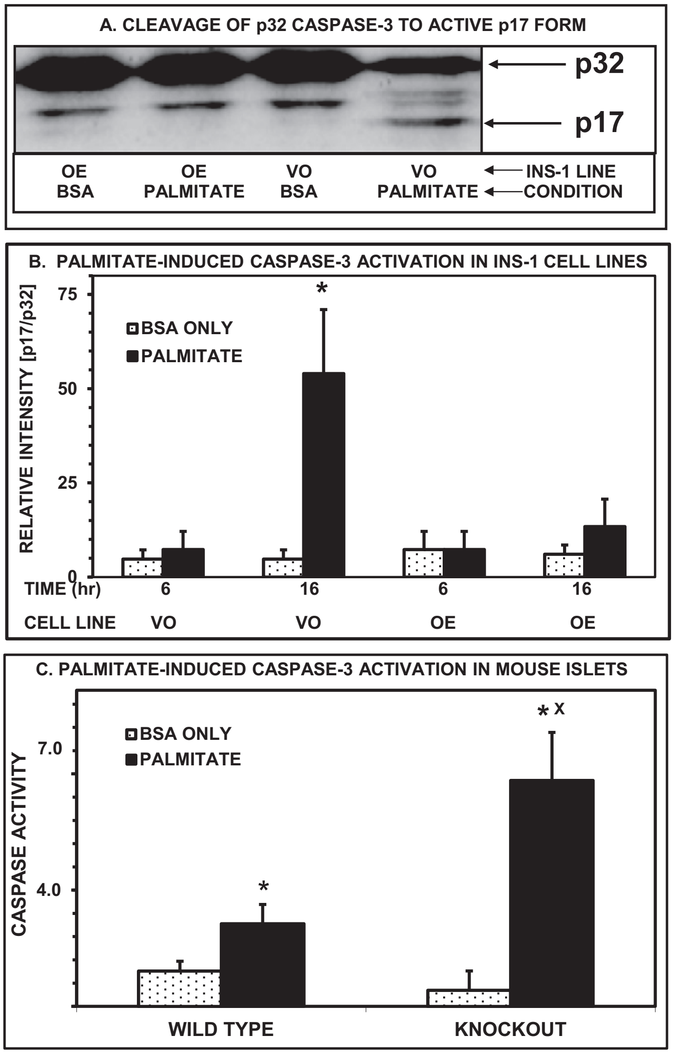

FIGURE 1. **Incubation of INS-1 cells and mouse pancreatic islets with palmitate induces caspase-3 activation that is inversely correlated with iPLA$_2\beta$ expression level.** In *A*, stably transfected iPLA$_2\beta$-OE INS-1 cells that overexpress (*OE*) iPLA$_2\beta$ or control cells transfected with vector only (*VO*) were incubated (6 or 16 h) in buffer that contained 1% BSA without or with 1 mM palmitate. Cells were then harvested, and their lysates were analyzed by SDS-PAGE and immunoblotting with antibody against caspase-3. *B* displays densitometric ratios for activated p17 and parent p32 forms of caspase-3 protein. Mean values ±S.E. (*error bars*) are indicated ($n = 4$). In *C*, pancreatic islets isolated from wild-type or iPLA$_2\beta$ knock-out mice were incubated (24 h) in buffer that contained 1% BSA without (*lightly stippled bars*) or with 1 mM palmitate (*solid black bars*). Caspase activity was then determined with a Caspase-Glo® 3/7 Assay kit. Mean values ±S.E. (*error bars*) are indicated ($n = 4$). An *asterisk* (*) denotes $p < 0.05$ for the difference between the BSA and palmitate conditions, and an *x* denotes a significant difference between wild type and knock-out.

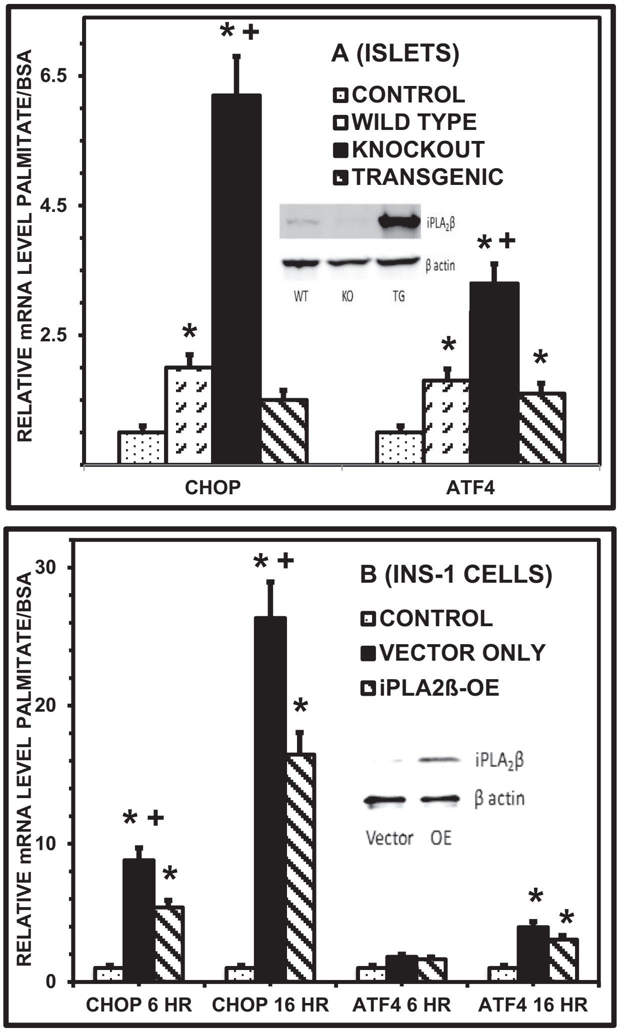

FIGURE 2. **Palmitate-induced expression of mRNA encoding transcription factors involved in endoplasmic reticulum stress by mouse pancreatic islets and INS-1 insulinoma cells correlates inversely with iPLA$_2\beta$ expression level.** In *A*, islets from wild type, iPLA$_2\beta$-null (*KNOCKOUT*), and transgenic mice that overexpress iPLA$_2\beta$ in β-cells were incubated (24 h) in buffer that contained 1% BSA without (*CONTROL*; *lightly stippled bars*) or with 1 mM palmitate (wild type, *finely cross-hatched bars*; knock-out, *solid black bars*; or transgenic, *coarsely cross-hatched bars*). RNA was then isolated, and cDNA was generated by RT-PCR. CHOP (*left set* of *bars*) and ATF4 (*right set* of *bars*) mRNA levels were measured by quantitative PCR and expressed as the ratio of the value for palmitate-treated cells divided by that for cells incubated in BSA buffer alone. Mean values ±S.E. (*error bars*) are indicated ($n = 4$). In *A*, an *asterisk* (*) denotes a significant ($p < 0.05$) increase over control, and a *plus* (+) denotes a significant difference from wild type. In *B*, iPLA$_2\beta$-OE or vector-only INS-1 cells were incubated (6 or 16 h) in buffer that contained 1% BSA without (*CONTROL*) or with 1 mM palmitate (*solid black bars* for vector-only and *cross-hatched bars* for iPLA$_2\beta$-OE cells). CHOP and ATF4 mRNA levels were measured by quantitative PCR and expressed as a ratio of values for palmitate-treated cells divided by that for cells incubated in BSA-buffer alone. Mean values ±S.E. (*error bars*) are indicated ($n = 4$). An *asterisk* (*) denotes a significant ($p < 0.05$) increase over control, and a *plus* (+) denotes a significant difference between vector-only and iPLA$_2\beta$-OE cells. *Inset* immunoblots illustrate relative iPLA$_2\beta$ expression levels in WT, KO, and TG islets (*A*) and vector-only and iPLA$_2\beta$-OE INS-1 cells (*B*), respectively.

Acentis Express C_8 column (150 × 2.1 mm, 5 μm) with a solvent gradient over 30 min from 32 to 97% solvent B (90% isopropanol, 10% acetonitrile, 10 mM ammonium formate) and from 68 to 3% solvent A (60% acetonitrile, 10 mM ammonium formate). Selected reaction monitoring was performed in negative ion mode. Collisionally activated dissociation of 4-HNE-DNPH was optimized at 24 eV in argon (1.0 millitorr). Transitions m/z 335 to m/z 182 and m/z 338 to m/z 182 were monitored for 4-HNE-DNPH and d_3-4HNE-DNPH, respectively.

Cardiolipin and Monolysocardiolipin Analyses by ESI/MS/MS—Internal standard (tetramyristoyl-cardiolipin ((C14:0)$_4$-CL)) was added to extracted lipids, and the mixture was concentrated, reconstituted, and infused into the ion source of an LTQ-Orbitrap Velos mass spectrometer (ThermoElectron) operated at a resolution of 30,000 with a maximum injection time of 50 ms (40). Alternatively, lipid extracts containing cardiolipin and/or monolysocardiolipin were analyzed by

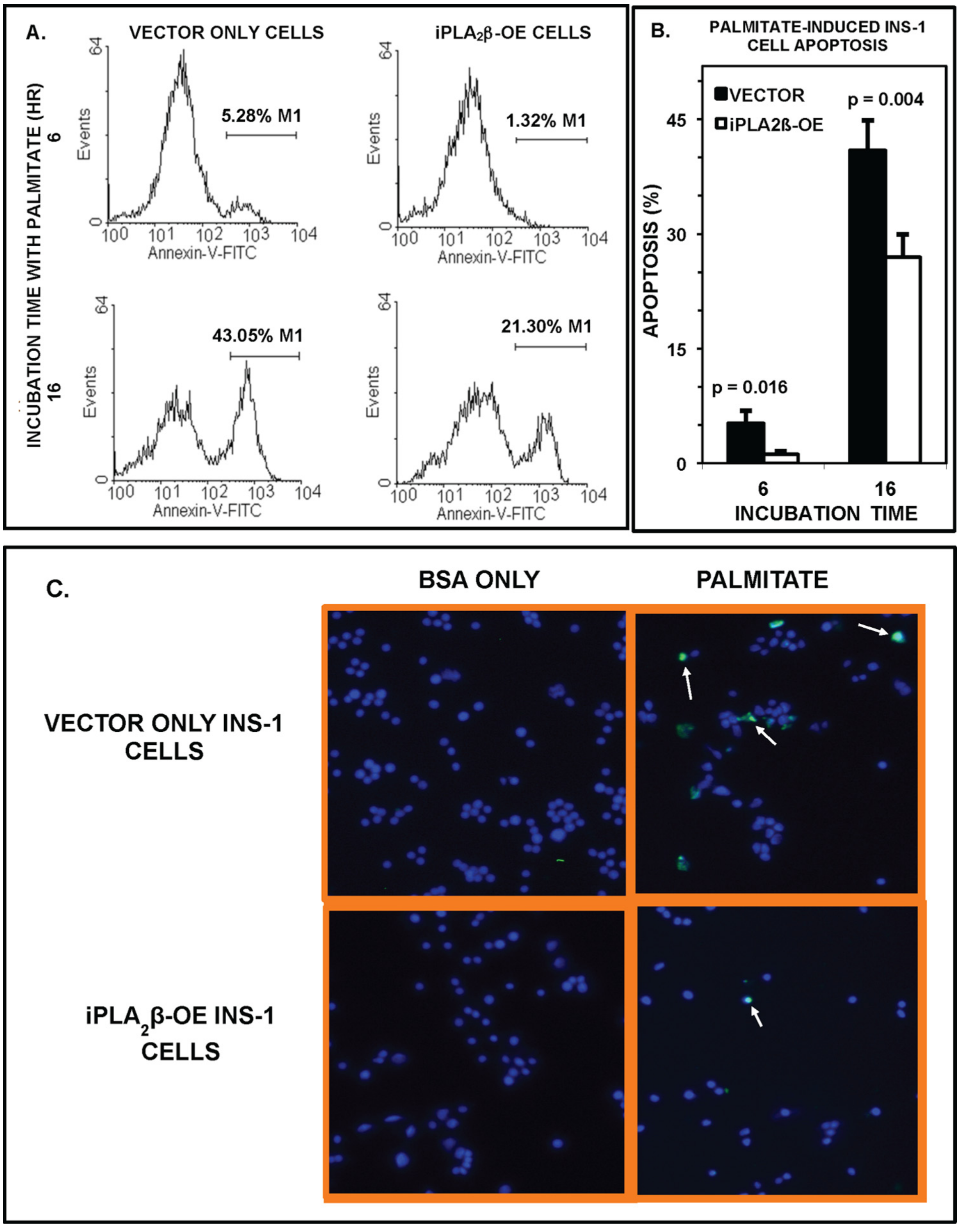

FIGURE 3. **Incubation with palmitate induces apoptosis of INS-1 cells, and overexpression of iPLA$_2\beta$ attenuates this effect.** iPLA$_2\beta$-OE (*light stippled bars*) or vector-only (*dark bars*) INS-1 cells were incubated (6 or 16 h) in buffer that contained 1% BSA without or with 1 mM palmitate. Cells were harvested, and apoptosis was determined by FACS using a kit with Annexin V-fluorescein that binds externalized phosphatidylserine of apoptotic cells (*A*). Population *M1* reflects apoptosis. *B* displays the increase in the percentage of apoptotic cells after incubation with palmitate compared with BSA alone. Mean values ±S.E. (*error bars*) are indicated ($n = 4$). Displayed *p* values reflect differences between vector-only and iPLA$_2\beta$-OE cells. *C* is an image from a TUNEL assay in which nuclei stain *blue* with DAPI and apoptotic cells stain *green* with TUNEL reagent as indicted by the *white arrows*.

LC/MS(/MS) in a manner similar to that described previously (41) on a Surveyor HPLC (ThermoElectron) using a modified gradient (42) on a C_8 column (15 cm × 2.1 mm; Sigma) interfaced with the ion source of a ThermoElectron Vantage triple quadruple mass spectrometer with extended mass range operated in negative ion mode.

Preparation of Oxidized Cardiolipin—As described (39), standard $(C18{:}2)_4$-CL was dissolved in chloroform in a glass vial and concentrated to dryness under nitrogen. PBS (100 μl; 50 mM, pH 7.4) with 100 μM diethylene triamine pentaacetic acid was then added, and the lipid mixture was Vortex-mixed and sonicated (10 min, under N_2, in water). Cytochrome *c* (20 μl; 200 μM) and H_2O_2 (20 μl; 250 μM) were then added, and the mixture was incubated (37 °C, under air, 1 h). During the incubation, H_2O_2 was added at 15-min intervals (final concentration, 100 μM). Lipid extraction was performed as above, and concentrated extracts were reconstituted (chloroform/methanol, 1:1, v/v; 200 μl) and analyzed by ESI/MS on a ThermoElectron TSQ Vantage triple quadrupole mass spectrometer in negative ion mode.

Cardiolipin Hydrolysis by iPLA$_2\beta$—Purified recombinant iPLA$_2\beta$ (2 μg) was added to hydrolysis buffer (50 μl; 200 mM Tris (pH 7.5) 5×, 20 mM EGTA) and diluted with homogenization buffer (0.25 M sucrose, 40 mM Tris (pH 7.5)) to achieve a 200-μl final volume. Standard $(C18{:}2)_4$-CL or oxidized CL in ethanol (5 μl) was then added, and the mixture was Vortex-

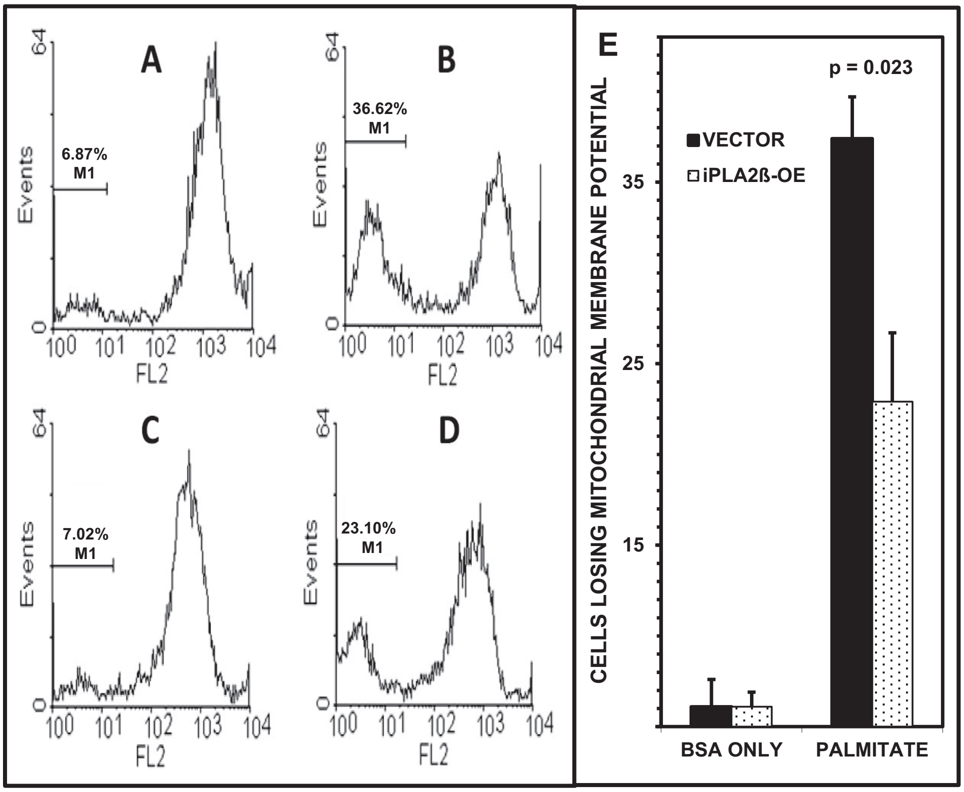

FIGURE 4. **Palmitate induces loss of INS-1 cell mitochondrial membrane potential, and this is blunted by overexpression of iPLA$_2\beta$.** IPLA$_2\beta$-OE (*C* and *D*) or control cells (*A* and *B*) were incubated (16 h) in buffer that contained 1% BSA without (*A* and C) or with 1 mM palmitate (*B* and *D*). Mitochondrial membrane potential was determined with a JC-1 Mitochondrial Membrane Potential Detection kit and FACS. A fall in mitochondrial potential results in a shift in JC-1 fluorescence from red to green as reflected by the *M1* population of cells (*A–D*). *E* displays the percentage of cells that lost mitochondrial membrane potential. Vector-only (*VECTOR*) cells are denoted by *solid black bars*, and iPLA$_2\beta$-OE cells are denoted by *light stippled bars*. Mean values ±S.E. (*error bars*) are indicated ($n = 4$). The displayed p value pertains to the difference between vector-only and iPLA$_2\beta$-OE cells.

mixed and incubated (37 °C, shaking water bath, 5 min). Lipids were extracted and analyzed by ESI/MS as above.

HPLC/ESI/MS/MS Analysis of Other Oxidized Phospholipids from INS-1 Cells—Lipids extracted from INS-1 cells were stored in sealed vials (under N_2 at −20 °C), and extracts were then analyzed by LC/MS/MS essentially as described (41) on a Surveyor HPLC (ThermoElectron) using a modified gradient (36) on a C_8 column (15 cm × 2.1 mm; Sigma) interfaced with the ion source of a ThermoElectron Vantage triple quadruple mass spectrometer with extended mass range operated in negative ion mode. Tandem MS scans for precursors of m/z 295, m/z 319, and m/z 343 were performed to identify glycerolipid molecular species that contained singly oxygenated forms of the polyunsaturated fatty acids (PUFAs) linoleate (C18:2), arachidonate (C20:4), and docosahexaenoate (C22:6), respectively. The major oxylipid species identified was (stearoyl, hydroxyeicosatetraenoyl)-glycerophosphoethanolamine ((C18:0/HETE)-GPE), and it was quantified by multiple reaction monitoring of the transition m/z 782.6 to m/z 319.3, reflecting production of HETE carboxylate anion from the parent oxyphospholipid $[M - H]^-$ ion.

Oxidation of C18:0/C20:4-GPE to C18:0/HETE-GPE and Its Hydrolysis by Recombinant iPLA$_2\beta$ to Yield Free HETE—Standard C18:0/C20:4-GPE was oxidized with H_2O_2/cytochrome *c* as described above for cardiolipin oxidation. After lipid extraction and concentration, samples were incubated (37 °C, 5 min) without or with recombinant iPLA$_2\beta$. After adding internal standards (C14:0/C14:0-GPE and [$^2H_8$]arachidonate), reaction mixtures were analyzed by ESI/MS from m/z 630 to m/z 800 and from m/z 308 to visualize substrate and product, respectively. Relevant $[M - H]^-$ m/z values are 634 (C14:0/C14:0-GPE), 782 (C18:0/HETE-GPE), 311 ([$^2H_8$]arachidonate), and 319 (HETE).

Statistical Analyses—Results are presented as mean ± S.E. Data were evaluated by unpaired, two-tailed Student's t test for differences between two conditions or by analysis of variance with appropriate post hoc tests for larger data sets (22). Significance levels are described in figure legends, and a p value <0.05 was considered significant.

RESULTS

Palmitate Induces Caspase-3 Activation and Other Markers of Cellular Injury in INS-1 Cells and in Mouse Pancreatic Islets, and the Magnitudes of These Effects Vary Inversely with iPLA$_2\beta$ Expression Level—Proteolytic activation of caspase-3, which is a key protease in the execution of apoptosis via the mitochondrial pathway (43), is reflected by generation of the active p17 product from its p32 precursor, and incubation with palmitate induced time-dependent activation of caspase-3 in INS-1 insulinoma cells stably transfected with vector only (Fig. 1*A*). Such activation was not observed with iPLA$_2\beta$-OE INS-1 cells that overexpress iPLA$_2\beta$ (Fig. 1*B*). (The preparation and properties of iPLA$_2\beta$-OE and vector-only INS-1 cells have been

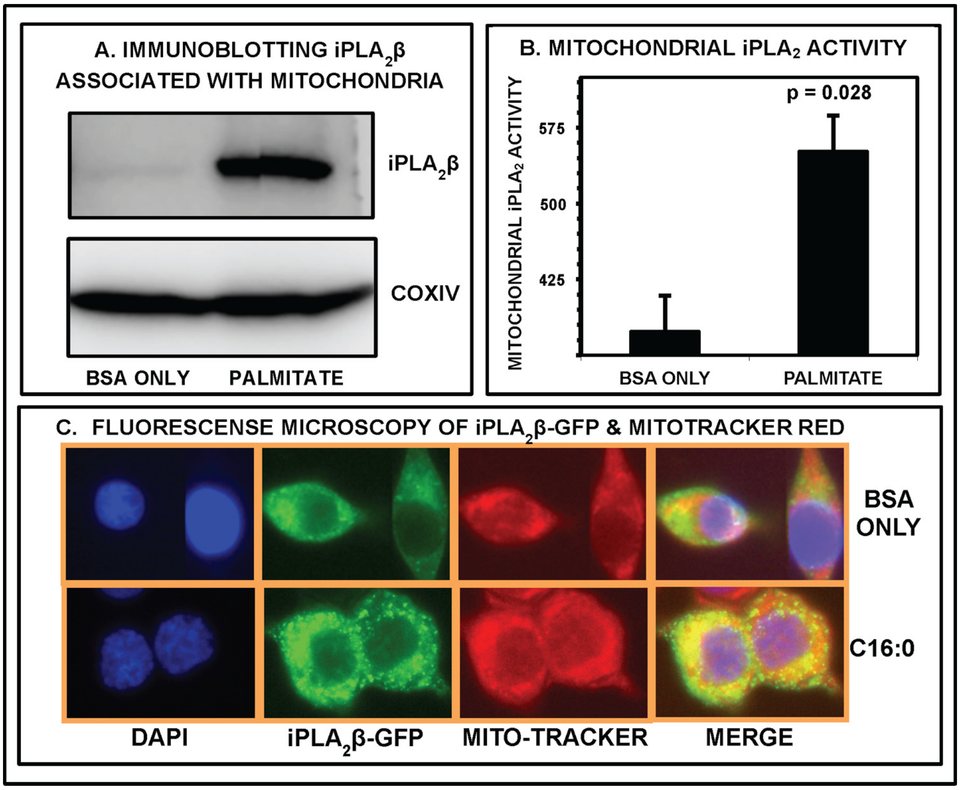

FIGURE 5. **Incubating INS-1 cells with palmitate results in subcellular redistribution of iPLA$_2\beta$ and its association with mitochondria.** In *A*, INS-1 cells were incubated (6 h) in buffer that contained 1% BSA without or with 1 mM palmitate. Mitochondrial and cytosolic fractions were then isolated, and mitochondrial proteins were analyzed by SDS-PAGE and immunoblotting with antibodies against iPLA$_2\beta$ and the mitochondrial protein COX IV. In *B*, mitochondrial Ca^{2+}-independent PLA$_2$ (*iPLA$_2$*) activity was measured by a radiochemical assay. Mean values ±S.E. (*error bars*) are indicated ($n = 4$). In *C*, INS-1 cells expressing iPLA$_2\beta$-GFP (*second lane*) were incubated (6 h) in buffer that contained 1% BSA without (*upper panels*) or with (*lower panels*) 1 mM C16:0. Cells were then loaded with MitoTracker Red (*third lane*) and DAPI (*first lane*) to mark mitochondria and nuclei, respectively, and examined by fluorescence microscopy. The *fourth lane* is the merged images of the *first three lanes*.

described previously (24, 29), and the differences in expression levels are illustrated in Fig. 2*B*, *inset*.) Caspase-3 activation was also examined by a more sensitive bioluminescence assay (31) in mouse pancreatic islets, which can be obtained in only limited quantities, and incubating iPLA$_2\beta$-KO islets with palmitate resulted in caspase-3 activation that was significantly greater than that for wild-type (WT) islets (Fig. 1*C*). (Generation and properties of KO mice have been described previously (25–27), and lack of iPLA$_2\beta$ expression is illustrated in Fig. 2*A*, *inset*.) Both INS-1 cell and islet data thus indicate that higher iPLA$_2\beta$ expression tends to confer protection against palmitate toxicity as reflected by caspase-3 activation.

Consistent with previous reports (11, 13, 44–49), incubation with palmitate also caused other manifestations of cellular injury in mouse pancreatic islets and INS-1 insulinoma cells (Fig. 2). These included accumulation of mRNA encoding ATF4 and CHOP (Fig. 2), which are transcription factors involved in endoplasmic reticulum stress-induced apoptosis, and accumulation of ceramide (supplemental Fig. S1), which is a mediator of fatty acid toxicity that inflicts mitochondrial injury and accumulates in β-cells undergoing apoptosis (4, 21, 50–52). Each of these responses was attenuated by overexpression of iPLA$_2\beta$ in INS-1 cells and amplified by iPLA$_2\beta$ deletion (Fig. 2 and supplemental Fig. S1), consistent with the protective effect of iPLA$_2\beta$ in palmitate-induced β-cell injury suggested by caspase-3 activation data (Fig. 1).

Overexpression of iPLA$_2\beta$ Reduces the Sensitivity of INS-1 Cells to Palmitate-induced Apoptosis—Caspase-3 activation is a harbinger of apoptosis, and to determine whether iPLA$_2\beta$ expression level affects palmitate-induced apoptosis of β-cells, the extent of apoptosis of INS-1 insulinoma cells incubated with palmitate was assessed by measuring phosphatidylserine externalization by apoptotic cells. iPLA$_2\beta$-OE INS-1 cells that overexpress iPLA$_2\beta$ were compared with cells transfected with empty vector only that express the lower levels of iPLA$_2\beta$ of the parental cell line. Cells were incubated with palmitate or vehicle and then treated with Annexin-FITC to impart fluorescence to cells that had externalized phosphatidylserine. The extent of apoptosis was then determined by flow cytometry as illustrated in Fig. 3*A* where the apoptotic cell populations are represented in the regions labeled *M1*. Incubation with palmitate induced a time-dependent increase in the percentage of cells that had undergone apoptosis, and this was significantly lower for iPLA$_2\beta$-OE INS-1 cells than for control INS-1 cells after both 6 and 16 h of incubation with palmitate (Fig. 3*B*). These data indicate that increased expression of iPLA$_2\beta$ by INS-1 cells confers a significant degree of protection against palmitate-induced apoptosis. (Similar results were obtained upon examination of cells that both bound Annexin and exhibited propidium iodide uptake (not shown), which reflects a late stage of apoptosis.)

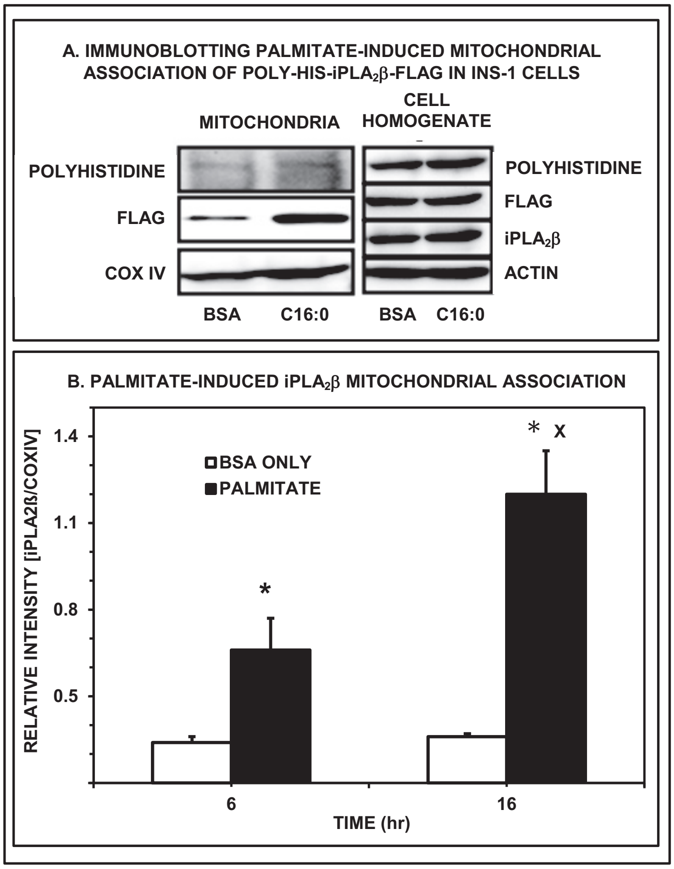

FIGURE 6. **The form of His-iPLA$_2\beta$-FLAG that associates with mitochondria in INS-1 cells incubated with palmitate retains a C-terminal FLAG tag but not an N-terminal polyhistidine tag.** In *A*, INS-1 cells expressing the fusion protein polyhisitidine-iPLA$_2\beta$-FLAG were incubated (6 or 16 h) in buffer containing 1% BSA without (*left lane*) or with (*right lane*) 1 mM palmitate. Mitochondrial and cytosolic fractions were then isolated from the cells, and mitochondrial proteins were analyzed by SDS-PAGE and immunoblotting with antibodies against FLAG, polyhistidine, or COX IV. *B* displays densitometric ratios of the signal for iPLA$_2\beta$-FLAG divided by that for COX IV at each condition. Mean values ±S.E. (*error bars*) are indicated ($n = 4$). An *asterisk* (*) indicates a significant ($p < 0.05$) difference between the palmitate and BSA-only conditions, and an *x* indicates a significant difference between 6- and 16-h time points.

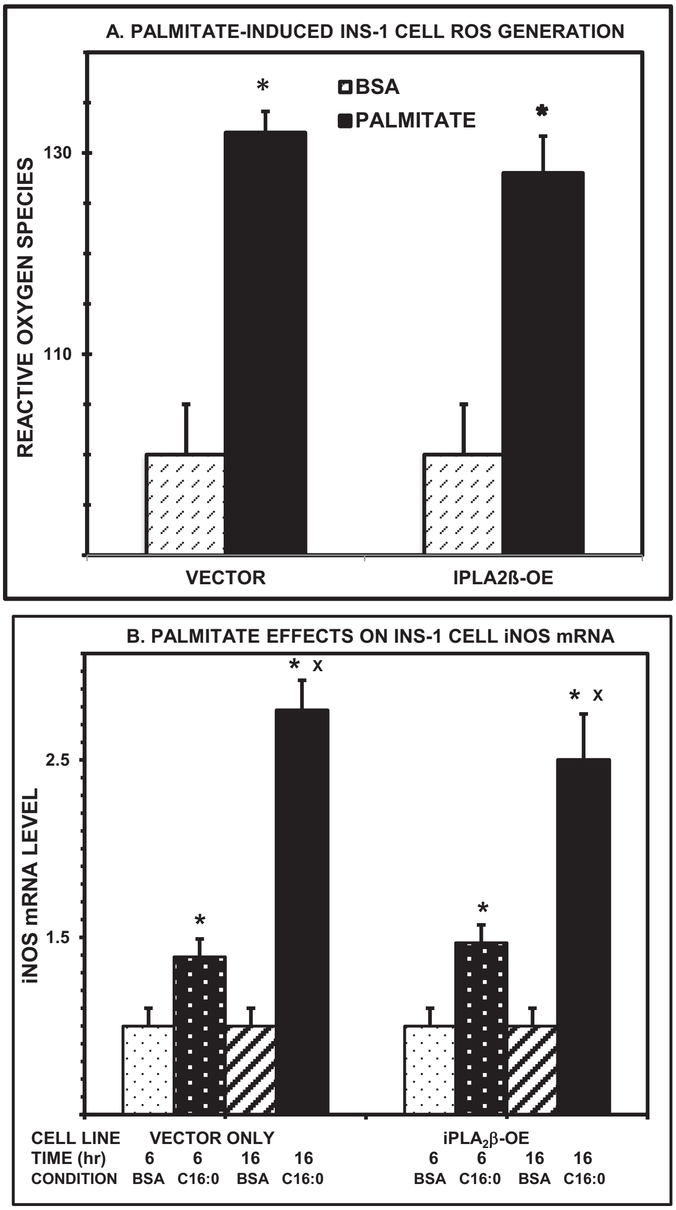

FIGURE 7. **Palmitate induces a rise in INS-1 cell reactive oxygen species and iNOS mRNA levels that is unaffected by overexpression of iPLA$_2\beta$.** iPLA$_2\beta$-OE or vector-only (*VECTOR*) INS-1 cells were incubated (16 h) in buffer that contained 1% BSA without or with 1 mM palmitate. In *A*, ROS were then measured with an OxiSelect assay as described under "Experimental Procedures." In *B*, after incubation, cellular iNOS mRNA content was measured by quantitative PCR. In both panels, mean values ±S.E. (*error bars*) are indicated ($n = 4$). An *asterisk* (*) denotes a significant ($p < 0.05$) difference between the palmitate (*solid black bars*) and BSA (*light cross-hatched* or *stippled bars*) conditions, and an *x* denotes a significant difference between 6- and 16-h time points. Differences between iPLA$_2\beta$-OE and vector-only cells were not significant in either *A* or *B*.

Overexpression of iPLA$_2\beta$ Attenuates Palmitate-induced INS-1 Cell Mitochondrial Membrane Potential Loss—$\Delta\Psi_m$ collapse is an early event in the apoptosis pathway that precedes phosphatidylserine externalization and coincides with caspase activation (53, 54), and the percentage of INS-1 cells with $\Delta\Psi_m$ collapse increased upon incubation with palmitate as reflected by fluorescence-activated cell sorting (FACS) of cells loaded with potential-sensitive indicator JC-1 (Fig. 4). Loss of $\Delta\Psi_m$ is reflected by signal in the region designated *M1* in Fig. 4, *A–D*, and after 16 h, that percentage was significantly lower for iPLA$_2\beta$-OE INS-1 cells than for control INS-1 cells, indicating that increased iPLA$_2\beta$ expression confers protection against palmitate-induced mitochondrial injury and loss of $\Delta\Psi_m$.

iPLA$_2\beta$ Undergoes Subcellular Redistribution upon Incubation of INS-1 Cells with Palmitate and Associates with Mitochondria—If protection of β-cells from palmitate toxicity reflects mitigation of mitochondrial injury as suggested by Fig. 4, then association of iPLA$_2\beta$ with mitochondria might be expected in cells incubated with palmitate. To examine this possibility, mitochondria were isolated from INS-1 cells, and their iPLA$_2\beta$ content was determined by immunoblotting and compared with that of the mitochondrial protein COX IV (22). Fig. 5*A* illustrates that incubating INS-1 cells with palmitate induced a marked increase in immunoreactive iPLA$_2\beta$ in the mitochondrial fraction relative to the BSA control, and there was a corresponding increase in Ca^{2+}-independent PLA$_2$ enzymatic activity associated with mitochondria (Fig. 5*B*). (Note that much of the iPLA$_2$ activity associated with mitochondria

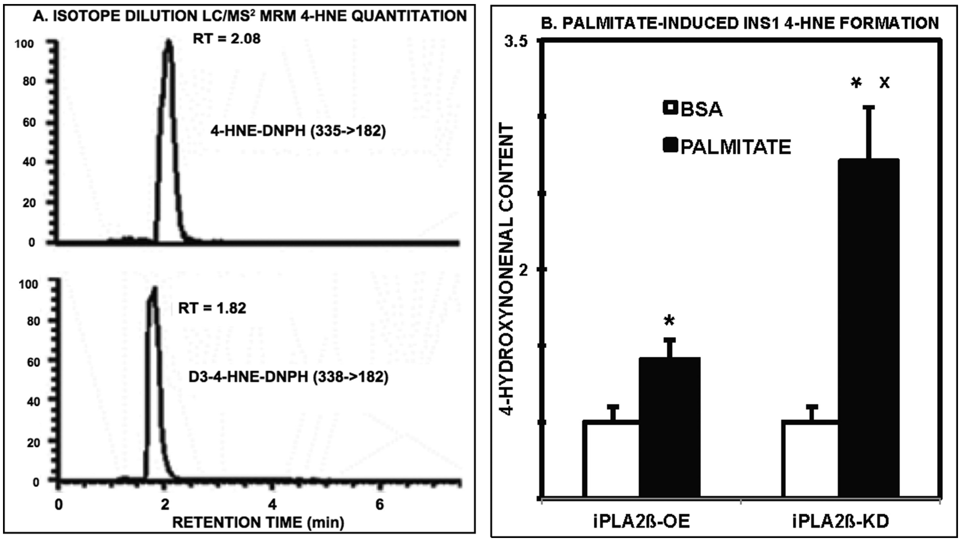

FIGURE 8. **Palmitate induces 4-HNE formation in INS-1 insulinoma cells.** *A* illustrates isotope dilution LC/MS/MS quantitation of the DNPH derivative of 4-HNE relative to the derivative of the internal standard d_3-4-HNE by monitoring the transitions *m/z* 335 to *m/z* 182 and *m/z* 338 to *m/z* 185, respectively. In *B*, iPLA$_2\beta$-OE (*left set* of *bars*) or iPLA$_2\beta$ knockdown (*KD*) (*right set* of *bars*) INS-1 cells were incubated (16 h) in buffer that contained 1% BSA without (*light cross-hatched bars*) or with 1 mM palmitate (*dark black bars*). Cellular lipids were then extracted, mixed with d_3-4-HNE, derivatized with DNPH, and analyzed by LC/MS/MS to determine 4-HNE content. Mean values ±S.E. (*error bars*) are indicated ($n = 4$). An *asterisk* (*) denotes a significant ($p < 0.05$) difference between BSA and palmitate conditions, and an *x* denotes a significant difference between iPLA$_2\beta$-OE and iPLA$_2\beta$ knockdown cells.

under basal conditions is attributable to the Group VIB PLA$_2$, also designated iPLA$_2\gamma$ (55).)

Subcellular distribution of iPLA$_2\beta$ was also examined by fluorescence microscopy in GFP-iPLA$_2\beta$ fusion protein-expressing INS-1 cells. In Fig. 5*C*, GFP-iPLA$_2\beta$ subcellular location is marked by *green* fluorescence and that of mitochondria is marked by *red* fluorescence from the MitoTracker indicator. Nuclei stain *blue* with the DAPI fluorescent indicator. iPLA$_2\beta$-GFP is uniformly distributed in the cytoplasm before incubation with palmitate (C16:0), and the INS-1 cells are spindle-shaped as illustrated in the *upper panel* (BSA control) of the *second lane* of Fig. 5*C*. After incubation with C16:0, INS-1 cells become rounded, and iPLA$_2\beta$-GFP *green* fluorescence displays a punctate distribution (Fig. 5*C*, *second lane*, *lower panel*). The *fourth lane* in Fig. 5*C* represents the merge of the *first three lanes*. It illustrates that the uniform *olive* hue of the extranuclear portion of cells incubated with BSA vehicle (Fig. 5*C*, *fourth lane*, *upper panel*) is replaced upon incubation with palmitate (Fig. 5*C*, *fourth lane*, *lower panel*) by an image with a punctate distribution of *yellow* spots from colocalized green and red signals from GFP-iPLA$_2\beta$ and MitoTracker, respectively, reflecting palmitate-induced iPLA$_2\beta$ redistribution of from cytosol to mitochondria.

Because iPLA$_2\beta$ undergoes proteolytic processing that affects its organellar association (35, 38, 56, 57), a His-iPLA$_2\beta$-FLAG fusion protein with N-terminal polyhistidine and C-terminal FLAG tags was expressed in INS-1 cells that were incubated with palmitate and then disrupted. Mitochondria were isolated, and their proteins were analyzed by SDS-PAGE and immunoblotting with antibodies against polyhistidine or FLAG or against mitochondrial COX IV (Fig. 6*A*, *left panel*). Cell homogenate was similarly analyzed with antibodies against polyhistidine or FLAG, iPLA$_2\beta$ internal sequence, or actin as controls (Fig. 6*A*, *right panel*). Mitochondrial immunoreactivity with anti-FLAG antibody at iPLA$_2\beta$-FLAG fusion protein molecular weight increased substantially in INS-1 cells incubated with palmitate (*Fig. 6A*, *left panel*, *middle blot*), but little such signal was obtained with anti-polyhistidine antibody (Fig. 6*A*, *left panel*, *top blot*), although signal was obtained with fusion protein-expressing INS-1 cell homogenates (Fig. 6*A*, *right panel*, *top blot*). Mitochondrial iPLA$_2\beta$-FLAG immunoreactivity increased with palmitate incubation interval (Fig. 6*B*). This suggests that the form of iPLA$_2\beta$ that C16:0 causes to associate with mitochondria is processed at the N terminus.

Palmitate Induces Phospholipid Oxidation in INS-1 Cells—Consistent with reports that palmitate toxicity in β-cells and other cells results from injury by ROS (8, 58–60), incubating INS-1 cells with palmitate was found to result in increased ROS generation as reflected by 2′,7′-dichlorodihydrofluorescin oxidation to the fluorescent 2′,7′-dichlorofluorescein, and there was no significant difference between control and iPLA$_2\beta$-OE INS-1 cells in that regard (Fig. 7*A*). Similarly, incubating INS-1 cells with palmitate induced a time-dependent rise in iNOS mRNA levels, consistent with reports that palmitate causes increased iNOS expression in β-cells and other cells (12, 58, 61–64), and there was no significant difference between control and iPLA$_2\beta$-OE INS-1 cells in the magnitude of that effect (Fig. 7*B*). Both ROS and NO can induce lipid oxidation in mitochondrial and other cellular membranes (65–68), and incubation with palmitate also induced a rise in INS-1 cell content of the lipid peroxidation product 4-HNE as demonstrated by a multiple reaction monitoring LS/MS/MS assay (Fig. 8). The magnitude of the rise in 4-HNE was inversely related to iPLA$_2\beta$ expression level (Fig. 8*B*), consistent with the possibility that iPLA$_2\beta$ excises oxidized linoleate residues from CL and that the yield of 4-HNE from linoleate oxidation is much greater for residues within tetralinoleoyl-CL ($(18:2)_4$-CL) species because intramolecular radical addition between neighboring linoleate chains amplifies 4-HNE formation (39).

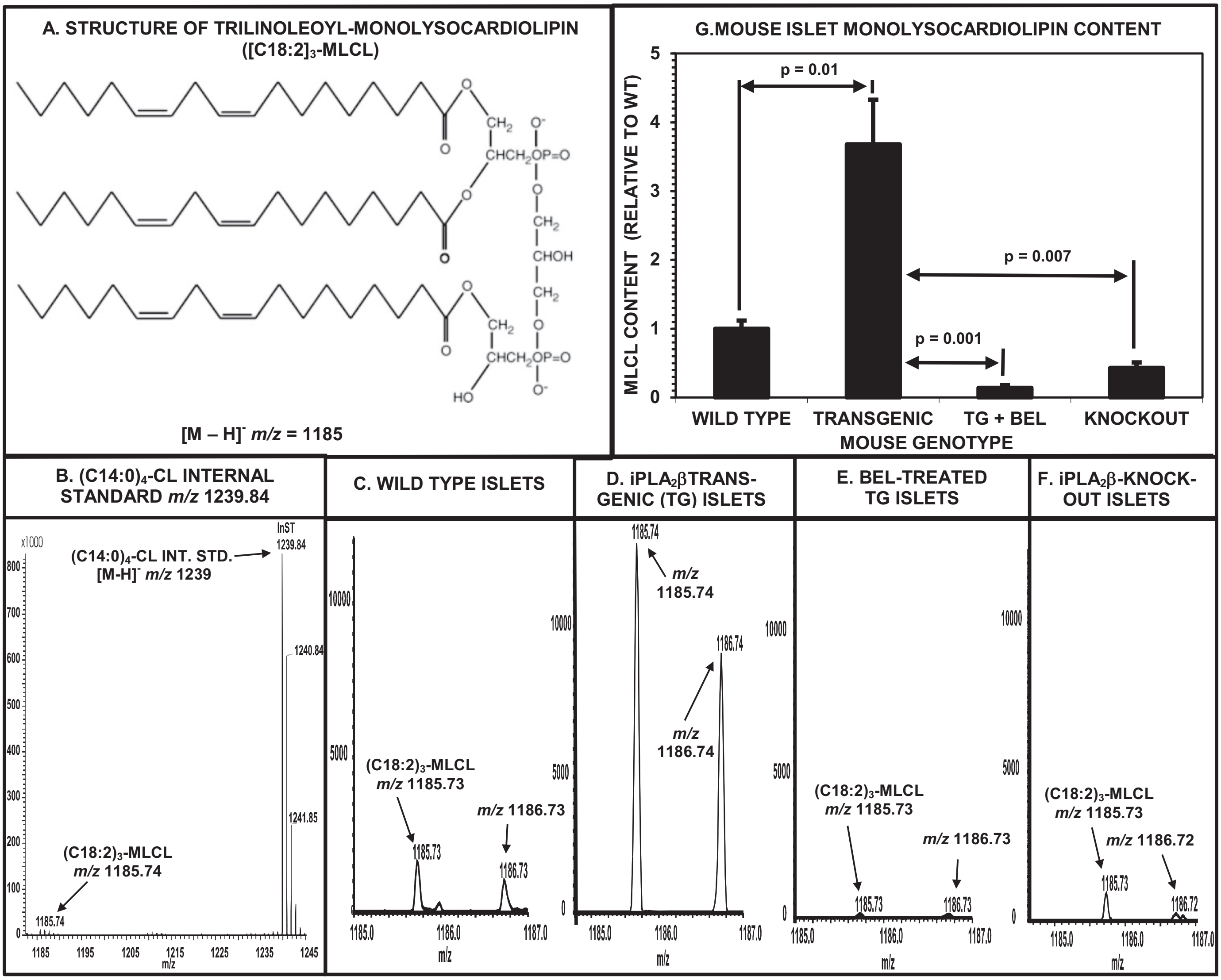

FIGURE 9. **The monolysocardiolipin content of pancreatic islets isolated from mice increases with the level of iPLA$_2\beta$ expression.** Pancreatic islets were isolated from WT, iPLA$_2\beta$-KO, and -TG mice that overexpress iPLA$_2\beta$ in β-cells, and their phospholipids were extracted, mixed with internal standard (C14:0)$_4$-CL, and analyzed for content of endogenous (C18:2)$_3$-MLCL by high resolution ESI/MS on an LTQ-Orbitrap Velos instrument. *A* is a structural diagram of (C18:2)$_3$-MLCL and specifies the nominal *m/z* value of its [M − H]$^-$ ion. *B* is an ESI/MS spectrum of the internal standard (C14:0)$_4$-CL that displays [M − H]$^-$, its first four ^{13}C isotopomers, and the small blank signal for (C18:2)$_3$-MLCL. *C–F* are high resolution partial mass spectra from islet samples that display the [M − H]$^-$ ion of (C18:2)$_3$-MLCL and its first ^{13}C isotopomer. Displayed signals are normalized for the intensity of the internal standard ion that is illustrated in *B* but is not displayed in *C–F*. Islet genotypes were: WT (*C*), iPLA$_2\beta$-TG (*D*), iPLA$_2\beta$-TG treated with the iPLA$_2\beta$ inhibitor bromoenol lactone (*BEL*) (*E*), and iPLA$_2\beta$-KO (*F*). *G* summarizes the relative content of (18:2)$_3$-MLCL in those four sets of samples. Mean values ±S.E. (*error bars*) and *p* values are indicated (n = 4).

The Monolysocardiolipin (MLCL) Content of Insulin-secreting β-Cells Rises with Increasing iPLA$_2\beta$ Expression Level, and iPLA$_2\beta$ Generates MLCL from CL—It has been proposed that iPLA$_2\beta$ confers resistance to oxidation-induced mitochondrial injury and apoptosis by excising oxidized linoleate residues from the mitochondrial phospholipid CL to generate MLCL that can be reacylated to regenerate native CL (19, 20, 69–74). To determine whether iPLA$_2\beta$ participates in β-cell MLCL metabolism, we quantified the trilinoleoyl-MLCL ((C18:2)$_3$-MLCL) species that is the precursor of the predominant mammalian CL species ((C18:2)$_4$-MLCL) by high resolution ESI/MS (40) relative to (C14:0)$_4$-CL internal standard. The content of (C18:2)$_3$-MLCL was determined in pancreatic islets isolated from WT and iPLA$_2\beta$-KO mice and from TG mice (27) that overexpress iPLA$_2\beta$ in β-cells. Fig. 9 illustrates that the (C18:2)$_3$-MLCL content is 3-fold higher in TG (*C*) than in WT (*A*) islets and that KO islets (*E*) contain less than half the (C18:2)$_3$-MLCL in WT islets. Moreover, pharmacologic inhibition of iPLA$_2\beta$ activity with the suicide substrate (73, 74) bromoenol lactone (*D*) results in a marked decline in TG islet (C18:2)$_3$-MLCL content (Fig. 9). Islet (C18:2)$_3$-MLCL content thus correlates positively with iPLA$_2\beta$ expression level and activity. This is consistent with the proposed role of iPLA$_2\beta$ in MLCL formation (70–72) as is the finding that recombinant iPLA$_2\beta$ converts standard (C18:2)$_4$-CL to (C18:2)$_3$-MLCL (Fig. 10).

Oxidized Cardiolipin Species Are Hydrolyzed by iPLA$_2\beta$ to Release Oxygenated Free Fatty Acids—To evaluate the proposal that iPLA$_2\beta$ participates in repairing oxidized CL by removing oxidized PUFA residues (8, 19, 20, 58–60, 70–72,

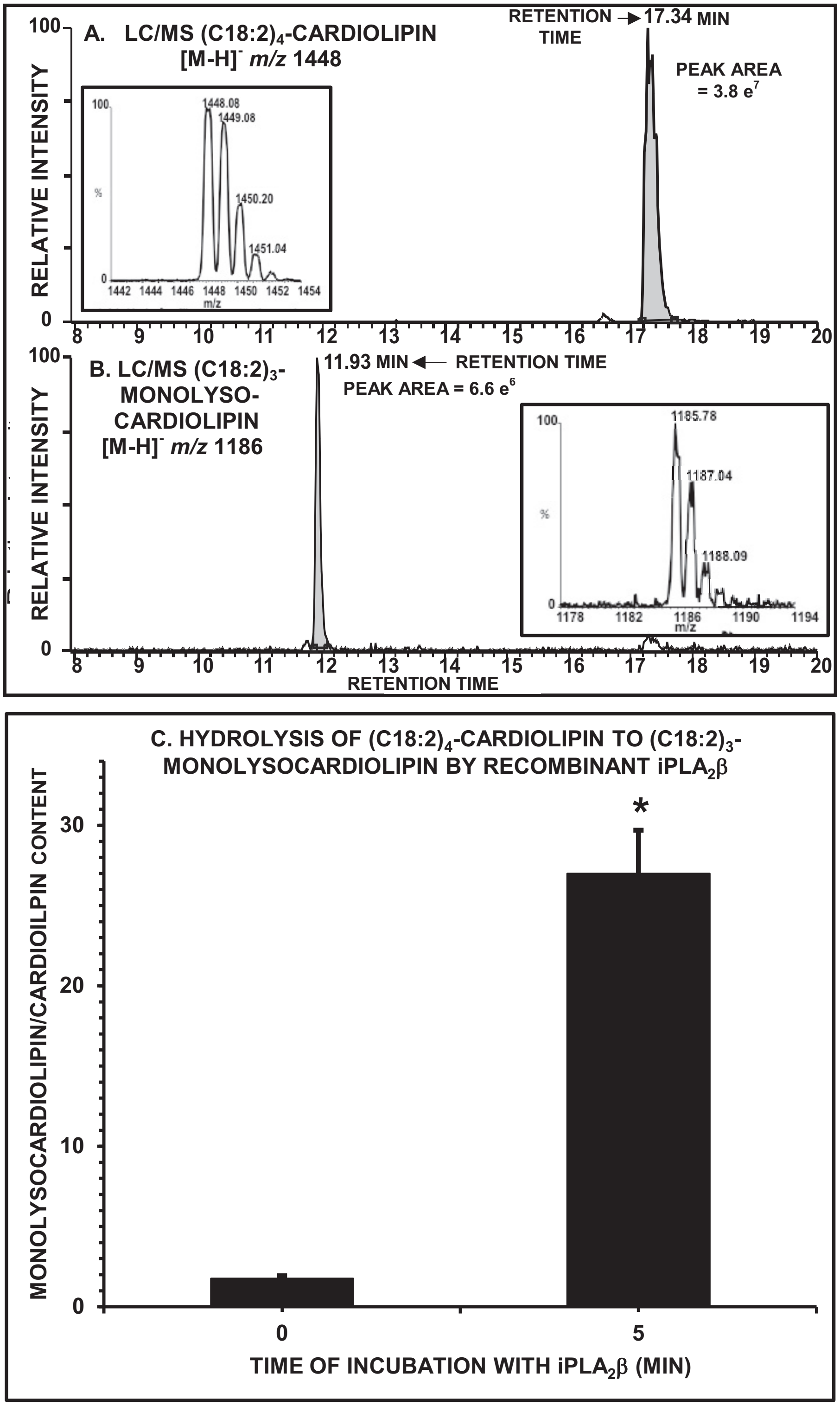

FIGURE 10. **iPLA$_2$β catalyzes hydrolysis of (C18:2)$_4$-cardiolipin to (C18:2)$_3$-monolysocardiolipin.** Recombinant iPLA$_2$β with an N-terminal polyhistidine sequence (His-iPLA$_2$β) was prepared and purified by immobilized metal affinity chromatography, and the protein content was determined by Coomassie assay. Standard bovine heart cardiolipin was incubated with His-iPLA$_2$β in hydrolysis buffer, and lipids were extracted and analyzed by HPLC/MS as illustrated in *A* and *B*. *A* depicts an HPLC/MS chromatogram obtained by selected monitoring of the (C18:2)$_4$-CL $[M - H]^-$ ion, and the *inset* is a full scan of the *m/z* region around $[M - H]^-$ to depict ^{13}C isotopomers. *B* depicts a similar analysis of (C18:2)$_3$-MLCL. *C* displays the ratio of ((C18:2)$_3$-MLCL/(C18:2)$_4$-CL) at time 0 and after 5 min of incubation with iPLA$_2$β as determined by HPLC/MS. Mean values ±S.E. (*error bars*) are indicated ($n = 4$). An *asterisk* (*) denotes a significant ($p < 0.05$) difference between the MLCL/CL values for 0- and 5-min time points.

75), standard (C18:2)$_4$-CL (Fig. 11*A*) was oxidized *in vitro* (Fig. 11*B*) with a cytochrome c/H_2O_2 system (40), and the oxidized CL preparation was incubated with recombinant iPLA$_2$β, which resulted in release of oxidized linoleate derivatives and native C18:2 (Fig. 11*C*). Quantitative LC/MS measurements of the time course of iPLA$_2$β-catalyzed fatty

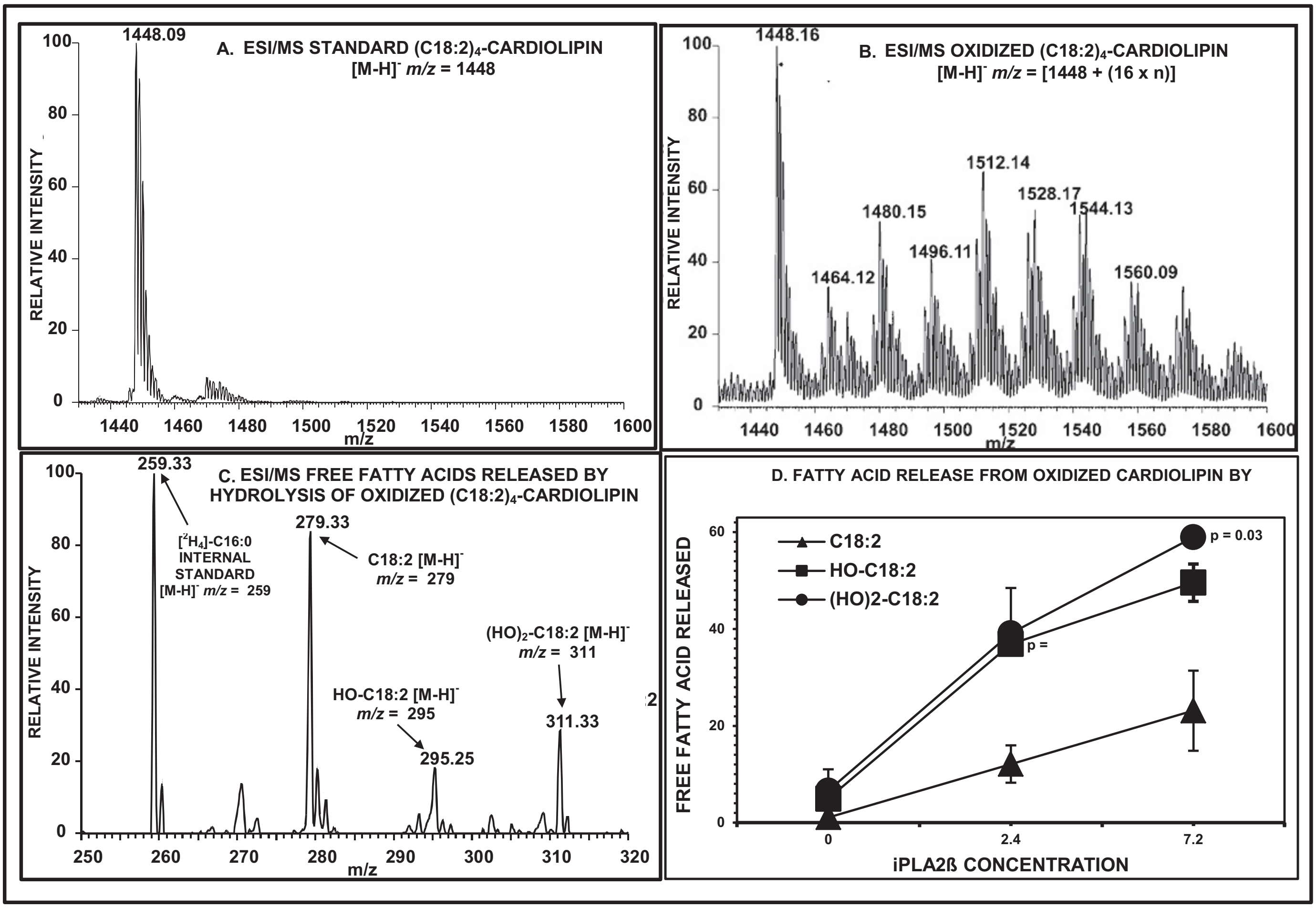

FIGURE 11. **iPLA$_2\beta$ catalyzes hydrolysis of oxidized (C18:2)$_4$-cardiolipin species to release oxygenated free fatty acids.** *A* is the negative ion ESI/MS spectrum of standard (C18:2)$_4$-CL that illustrates the $[M-H]^-$ ion and its ^{13}C isotopomers and little signal in the region from *m/z* 1460 to *m/z* 1600, and *B* is a spectrum after oxidation with cytochrome *c*/H_2O_2 that illustrates formation of multiple oxidation products reflected by peaks with *m/z* values of $1448 + (n \times 16)$ where $n = 1–8$. *C* is the ESI/MS spectrum from *m/z* 250 to *m/z* 320 of the lipid extract of an incubation mixture of partially oxidized CL and His-iPLA$_2\beta$ under the conditions in Fig. 6, and it illustrates $[M-H]^-$ ions of the internal standard [$^2H_4$]palmitate (d_4-C16:0, *m/z* 259), linoleate (C18:2, *m/z* 279), oxylinoleate (O-C18:2, *m/z* 295), and dioxylinoleate (O_2-C18:2, *m/z* 311). *D* summarizes the time course of iPLA$_2\beta$-catalyzed release of free fatty acids from oxidized CL. Mean values ±S.E. (*error bars*) are indicated. Displayed values pertain to differences between the indicated fatty acid and C18:2 at various time points.

acid release indicated that oxidized residues were released more readily than native C18:2 (Fig. 11*D*), consistent with the proposed role of iPLA$_2\beta$ in repairing oxidized mitochondrial phospholipids (19, 20, 70–72, 75).

Oxidized Phospholipids Accumulate in β-Cells Incubated with Palmitate, and This Is Attenuated by iPLA$_2\beta$ Overexpression—Consistent with reports that ROS contribute to palmitate toxicity (8, 65–68, 75) and oxidize lipids in mitochondrial and other cellular membranes (65–68, 75), oxidized CL (oxy-CL) species were observed by LC/MS (Fig. 12, *A* and *B*) to accumulate in control INS-1 cells incubated with palmitate (Fig. 12*C*). In contrast, no significant palmitate-induced oxy-CL accumulation occurred in iPLA$_2\beta$-OE INS-1 cells (Fig. 12*C*), consistent with the proposed iPLA$_2\beta$ role to remove oxidized PUFA substituents from oxy-CL to yield MLCL (Figs. 9–11). Mitochondria also contain substantial amounts of GPE lipids, which undergo the largest fractional modification among mitochondrial lipid classes upon induction of apoptosis (22). LC/ESI/MS/MS scanning for parent ions that liberate an oxidized PUFA carboxylate anion (supplemental Fig. S2A) upon collisionally activated dissociation (41) revealed that HETE (*m/z* 319.3) from oxidized C18:0/C20:4-GPE (*m/z* 782.69) is the most abundant oxy-PUFA in INS-1 cells, consistent with reports that this is also the most abundant oxy-GPE lipid in platelets (41) and that C18:0/C20:4-GPE is the most abundant GPE lipid species in INS-1 cells and islets (29, 76). Supplemental Fig. S2B illustrates an MS/MS scan monitoring parent ions that generate HETE anion (*m/z* 319.3). The tandem spectrum of the vastly predominant parent (*m/z* 782.69) identifies the (C18:0/HETE)-GPE $[M-H]^-$ ion, and INS-1 cell (C18:0/HETE)-GPE content was quantified by LC/ESI/MS/MS scanning of the transition *m/z* 782.69 to *m/z* 319.3 (supplemental Fig. S2C). Incubation with palmitate induced a 4.2-fold increase in control INS-1 cell (C18:0/HETE)-GPE content but a much smaller rise in iPLA$_2\beta$-OE INS-1 cells (supplemental Fig. S2D), again consistent with the proposal that iPLA$_2\beta$ excises oxidized PUFA residues from phospholipids (19, 20). Recombinant iPLA$_2\beta$ was also found to catalyze release of HETE residues from C18:0/HETE-GPE prepared by oxidation of standard C18:0/20:4-GPE with H_2O_2 and cytochrome *c* (supplemental Fig. S3).

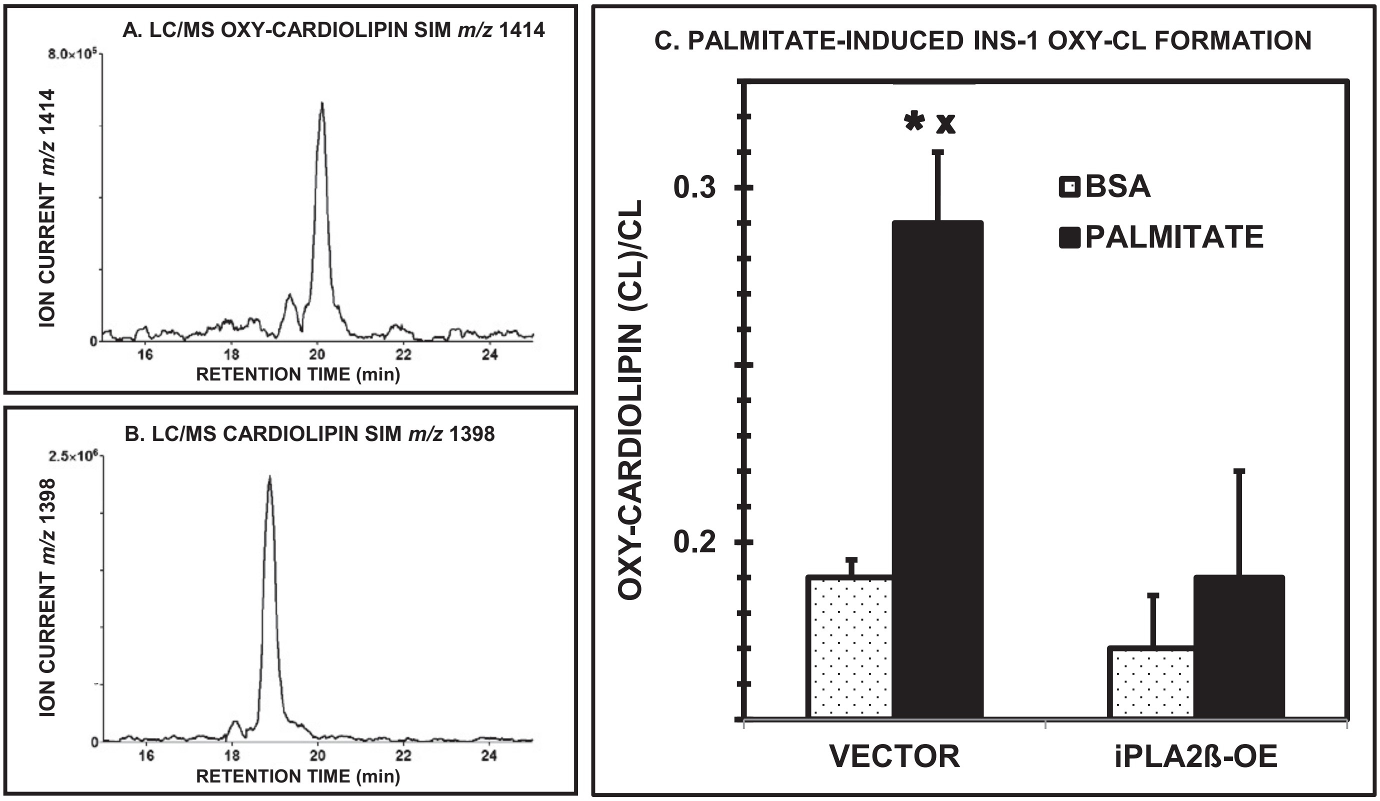

FIGURE 12. **Palmitate induces accumulation of an oxycardiolipin species in INS-1 cells, and this is attenuated by overexpression of iPLA$_2\beta$.** iPLA$_2\beta$-OE and vector-only INS-1 cells were incubated (16 h) in buffer that contained 1% BSA without (*light stippled bars*) or with 1 mM palmitate (*solid black bars*), and their lipids were extracted and analyzed by ESI/MS. *A* is an LC/MS tracing from selected ion monitoring of *m/z* 1398, which is the $[M - H]^-$ ion of (C16:0/C16:0/C18:1/C18:2)-CL. *B*, same as *A* but for (C16:0/C16:0/C18:1/hydroxy-C18:2)-CL. *C* summarizes the relative abundance of *m/z* 1414/*m/z* 1398 in vector-only (*VECTOR*) and iPLA$_2\beta$-OE INS-1 cells incubated without or with palmitate to illustrate palmitate-induced accumulation of the oxy-CL species. Mean values ±S.E. (*error bars*) are indicated ($n = 4$). An *asterisk* (*) denotes a significant ($p < 0.05$) difference between BSA and palmitate conditions, and an *x* denotes a significant difference between vector-only and iPLA$_2\beta$-OE INS-1 cells.

DISCUSSION

Apoptosis contributes to β-cell loss in the development of type 2 diabetes mellitus, and fatty acid toxicity participates in these processes by incompletely understood mechanisms. Generation of ROS by mitochondria has also been proposed to contribute to palmitate toxicity to cells (59), including β-cells (8–10), and prolonged β-cell exposure to high FFA concentrations does cause ROS production (8, 49, 77). Palmitate is reported to cause β-cell apoptosis by affecting fission and fusion of mitochondrial membranes (78, 79), and iPLA$_2\beta$ also affects mitochondrial membranes (19, 20, 22) and is proposed to participate in their repair from oxidative injury inflicted by ROS (73, 74). Our findings indicate that palmitate-induced mitochondrial injury in β-cells as reflected by collapse of $\Delta\Psi_m$ is mitigated by overexpressing iPLA$_2\beta$ in INS-1 cells, and iPLA$_2\beta$ may thus act to restrain the mitochondrial pathway of apoptosis.

Association of iPLA$_2\beta$ with mitochondria could mitigate injury from ROS by repairing oxidized mitochondrial phospholipids, such as CL. CL is critical for mitochondrial function and retention of cytochrome *c*, a mobile carrier required for electron transfer chain function (80–87). Interaction with cytochrome *c* depends upon CL C18:2 substituents, and a decline in inner mitochondrial membrane CL content or alteration of its C18:2 substituents resulting from defective CL remodeling or oxidative modification (84, 87) diminishes cytochrome *c* membrane affinity (87, 88). The resultant release of cytochrome *c* into the cytosol can precipitate apoptosis (86).

iPLA$_2\beta$ may participate in generating and maintaining the C18:2-rich composition of CL under physiologic and pathophysiologic conditions. Newly synthesized CL must be remodeled to produce mature C18:2-rich CL, and the mitochondrial enzymes MLCL acyltransferase and tafazzin appear to cooperate with a PLA$_2$ in this process. To remodel nascent CL, the substrate MLCL must be generated so that reacylation with linoleate can occur, and a Group VI PLA$_2$, *e.g.* iPLA$_2\beta$, iPLA$_2\gamma$, or both (55, 89–92), may catalyze MLCL formation. iPLA$_2\beta$ may play a role in repairing oxidized CL (19, 20, 70–72, 75) under pathophysiological circumstances that is similar to its proposed role in physiological CL remodeling. C18:2 residues are especially susceptible to oxidation because they contain bisallylic methylene moieties with a labile hydrogen atom that can be abstracted to yield a carbon-centered radical that readily reacts with molecular oxygen to form a fatty acid hydroperoxide (93). Oxidization reduces hydrophobicity of the fatty acid substituent and allows it to approach the hydrophilic phospholipid headgroup more closely (93). This increases separation between headgroups, causing the ester bond to be more accessible to PLA$_2$.

Group VI PLA$_2$ enzymes may participate in such repair of oxidized mitochondrial membrane phospholipids (19, 20, 73, 94–96). iPLA$_2\beta$ localizes to mitochondria in insulinoma cells and protects against oxidant-induced apoptosis, and pancreatic islets from iPLA$_2\beta$-null mice exhibit increased susceptibility to oxidant-induced apoptosis (19, 20, 73). Oxidant-induced lipid peroxidation and death of renal proximal tubule cells are potentiated by bromoenol lactone (95), which inhibits Group VI PLA$_2$ enzymes (97, 98). This may reflect iPLA$_2\beta$-catalyzed removal of oxidized PUFA residues from mitochondrial glycerophospholipids formed during oxidative stress. This would permit the resultant lysophospholipid to be reacylated with an unoxidized PUFA residue to restore functions impaired as a result of membrane oxidation. In the absence of iPLA$_2\beta$ or when its activity is reduced, this repair mechanism would not be fully operative, and this could result in progressive mitochondrial injury that eventually triggers the mitochondrial pathway of apoptosis (90–92). Conversely, increased iPLA$_2\beta$ activity might confer increased resistance to oxidative injury that would otherwise result in apoptosis and that is consistent with the protection against palmitate-induced apoptosis of INS-1 cells conferred by overexpression of iPLA$_2\beta$ demonstrated here.

Our findings indicate that β-cell MLCL content rises with increasing iPLA$_2\beta$ expression level, which is compatible with a role for iPLA$_2\beta$ in CL remodeling by excising oxidized PUFA residues from CL to yield MLCL species for reacylation with unoxidized C18:2-CoA to regenerate the native CL structure and function. This would stabilize the association of cytochrome *c* with mitochondrial membranes and mitigate ROS injury that would otherwise induce apoptosis (87). Our observations that the β-cell content of oxidized lipids rises after incubation with palmitate is consistent with the proposal that palmitate toxicity involves generation of ROS (8, 12, 49, 59, 63), and the correlation of these effects with iPLA$_2\beta$ expression level is consistent with the possibility that iPLA$_2\beta$ participates in an excision-reacylation repair mechanism for reducing membrane oxidized lipid content.

This proposed role for iPLA$_2\beta$ in repair of oxidized phospholipids represents a special case of the originally proposed function of the enzyme in phospholipid remodeling (99–102) and is consistent with the observations that oxidation of membranes accelerates iPLA$_2\beta$-catalyzed fatty acid release from membranes and that iPLA$_2\beta$ mediates oxidant-induced arachidonic acid release from cells (103–105). Moreover, iPLA$_2\beta$ is active against phospholipids with short chain *sn*-2 substituents (106), such as those produced from polyunsaturated fatty acids by oxidation reactions (107). These are also properties of the Group VII platelet-activating factor acetylhydrolase enzymes (101, 108), some of which have been have been proposed to function physiologically in clearance and/or repair of oxidized phospholipids (109). A similar role of a Group VI PLA$_2$, such as iPLA$_2\beta$, is plausible (109), and it is of interest in that regard that a plant analog of the mammalian Group VI PLA$_2$ enzymes designated patatin-containing phospholipase A (pPLAIIα) has been proposed to negatively regulate oxylipin production and to effect removal of oxidized fatty acids from the membranes of *Arabidopsis thaliana* (110).

Acknowledgments—We thank Robert Sanders and Susan Schumacher for assistance in preparing the manuscript and figures and Alan Bohrer for technical assistance.

REFERENCES

1. Reaven, G. M., Hollenbeck, C., Jeng, C. Y., Wu, M. S., and Chen, Y. D. (1988) Measurement of plasma glucose, free fatty acid, lactate, and insulin for 24 h in patients with NIDDM. *Diabetes* **37,** 1020–1024
2. Leonardi, O., Mints, G., and Hussain, M. A. (2003) β-Cell apoptosis in the pathogenesis of human type 2 diabetes mellitus. *Eur. J. Endocrinol.* **149,** 99–102
3. Rachek, L. I., Thornley, N. P., Grishko, V. I., LeDoux, S. P., and Wilson, G. L. (2006) Protection of INS-1 cells from free fatty acid-induced apoptosis by targeting hOGG1 to mitochondria. *Diabetes* **55,** 1022–1028
4. Shimabukuro, M., Zhou, Y. T., Levi, M., and Unger, R. H. (1998) Fatty acid-induced β cell apoptosis: a link between obesity and diabetes. *Proc. Natl. Acad. Sci. U.S.A.* **95,** 2498–2502
5. Cnop, M., Hannaert, J. C., Hoorens, A., Eizirik, D. L., and Pipeleers, D. G. (2001) Inverse relationship between cytotoxicity of free fatty acids in pancreatic islet cells and cellular triglyceride accumulation. *Diabetes* **50,** 1771–1777
6. Lupi, R., Dotta, F., Marselli, L., Del Guerra, S., Masini, M., Santangelo, C., Patané, G., Boggi, U., Piro, S., Anello, M., Bergamini, E., Mosca, F., Di Mario, U., Del Prato, S., and Marchetti, P. (2002) Prolonged exposure to free fatty acids has cytostatic and pro-apoptotic effects on human pancreatic islets: evidence that β-cell death is caspase mediated, partially dependent on ceramide pathway, and Bcl-2 regulated. *Diabetes* **51,** 1437–1442
7. Maedler, K., Spinas, G. A., Dyntar, D., Moritz, W., Kaiser, N., and Donath, M. Y. (2001) Distinct effects of saturated and monounsaturated fatty acids on β-cell turnover and function. *Diabetes* **50,** 69–76
8. Carlsson, C., Borg, L. A., and Welsh, N. (1999) Sodium palmitate induces partial mitochondrial uncoupling and reactive oxygen species in rat pancreatic islets *in vitro*. *Endocrinology* **140,** 3422–3428
9. Evans, J. L., Goldfine, I. D., Maddux, B. A., and Grodsky, G. M. (2003) Are oxidative stress-activated signaling pathways mediators of insulin resistance and β-cell dysfunction? *Diabetes* **52,** 1–8
10. Maestre, I., Jordán, J., Calvo, S., Reig, J. A., Ceña, V., Soria, B., Prentki, M., and Roche, E. (2003) Mitochondrial dysfunction is involved in apoptosis induced by serum withdrawal and fatty acids in the β-cell line INS-1. *Endocrinology* **144,** 335–345
11. Lai, E., Bikopoulos, G., Wheeler, M. B., Rozakis-Adcock, M., and Volchuk, A. (2008) Differential activation of ER stress and apoptosis in response to chronically elevated free fatty acids in pancreatic β-cells. *Am. J. Physiol. Endocrinol. Metab.* **294,** E540–E550
12. Meidute Abaraviciene, S., Lundquist, I., Galvanovskis, J., Flodgren, E., Olde, B., and Salehi, A. (2008) Palmitate-induced β-cell dysfunction is associated with excessive NO production and is reversed by thiazolidinedione-mediated inhibition of GPR40 transduction mechanisms. *PLoS One* **3,** e2182
13. Kharroubi, I., Ladrière, L., Cardozo, A. K., Dogusan, Z., Cnop, M., and Eizirik, D. L. (2004) Free fatty acids and cytokines induce pancreatic β-cell apoptosis by different mechanisms: role of nuclear factor-κB and endoplasmic reticulum stress. *Endocrinology* **145,** 5087–5096
14. Karaskov, E., Scott, C., Zhang, L., Teodoro, T., Ravazzola, M., and Volchuk, A. (2006) Chronic palmitate but not oleate exposure induces endoplasmic reticulum stress, which may contribute to INS-1 pancreatic β-cell apoptosis. *Endocrinology* **147,** 3398–3407
15. Laybutt, D. R., Preston, A. M., Akerfeldt, M. C., Kench, J. G., Busch, A. K., Biankin, A. V., and Biden, T. J. (2007) Endoplasmic reticulum stress contributes to β cell apoptosis in type 2 diabetes. *Diabetologia* **50,** 752–763
16. Xu, M., Wang, W., Frontera, J. R., Neely, M. C., Lu, J., Aires, D., Hsu, F. F., Turk, J., Swerdlow, R. H., Carlson, S. E., and Zhu, H. (2011) Ncb5or deficiency increases fatty acid catabolism and oxidative stress. *J. Biol. Chem.* **286,** 11141–11154
17. Wang, W., Guo, Y., Xu, M., Huang, H. H., Novikova, L., Larade, K., Jiang, Z. G., Thayer, T. C., Frontera, J. R., Aires, D., Ding, H., Turk, J., Mathews, C. E., Bunn, H. F., Stehno-Bittel, L., and Zhu, H. (2011) Development of diabetes in lean Ncb5or-null mice is associated with manifestations of endoplasmic reticulum and oxidative stress in β cells. *Biochim. Biophys. Acta* **1812,** 1532–1541

18. Guo, Y., Xu, M., Deng, B., Frontera, J. R., Kover, K. L., Aires, D., Ding, H., Carlson, S. E., Turk, J., Wang, W., and Zhu, H. (2012) β-Cell injury in Ncb5or-null mice is exacerbated by consumption of a high-fat diet. *Eur. J. Lipid Sci. Technol.* **114,** 233–243
19. Seleznev, K., Zhao, C., Zhang, X. H., Song, K., and Ma, Z. A. (2006) Calcium-independent phospholipase A_2 localizes in and protects mitochondria during apoptotic induction by staurosporine. *J. Biol. Chem.* **281,** 22275–22288
20. Zhao, Z., Zhang, X., Zhao, C., Choi, J., Shi, J., Song, K., Turk, J., and Ma, Z. A. (2010) Protection of pancreatic β-cells by group VIA phospholipase A_2-mediated repair of mitochondrial membrane peroxidation. *Endocrinology* **151,** 3038–3048
21. Ramanadham, S., Hsu, F. F., Zhang, S., Jin, C., Bohrer, A., Song, H., Bao, S., Ma, Z., and Turk, J. (2004) Involvement of the group VIA phospholipase A_2 (iPLA$_2\beta$) in endoplasmic reticulum stress-induced apoptosis in insulinoma cells. *Biochemistry* **43,** 918–930
22. Bao, S., Li, Y., Lei, X., Wohltmann, M., Jin, W., Bohrer, A., Semenkovich, C. F., Ramanadham, S., Tabas, I., and Turk, J. (2007) Attenuated free cholesterol loading-induced apoptosis but preserved phospholipid composition of peritoneal macrophages from mice that do not express group VIA phospholipase A_2. *J. Biol. Chem.* **282,** 27100–27114
23. Song, H., Wohltmann, M., Tan, M., Bao, S., Ladenson, J. H., and Turk, J. (2012) Group VIA PLA2 (iPLA2β) is activated upstream of p38 mitogen-activated protein kinase (MAPK) in pancreatic islet β-cell signaling. *J. Biol. Chem.* **287,** 5528–5541
24. Ma, Z., Ramanadham, S., Wohltmann, M., Bohrer, A., Hsu, F. F., and Turk, J. (2001) Studies of insulin secretory responses and of arachidonic acid incorporation into phospholipids of stably transfected insulinoma cells that overexpress group VIA phospholipase A_2 (iPLA$_2\beta$) indicate a signaling rather than a housekeeping role for iPLA$_2\beta$. *J. Biol. Chem.* **276,** 13198–13208
25. Bao, S., Miller, D. J., Ma, Z., Wohltmann, M., Eng, G., Ramanadham, S., Moley, K., and Turk, J. (2004) Male mice that do not express group VIA phospholipase A_2 produce spermatozoa with impaired motility and have greatly reduced fertility. *J. Biol. Chem.* **279,** 38194–38200
26. Bao, S., Song, H., Wohltmann, M., Ramanadham, S., Jin, W., Bohrer, A., and Turk, J. (2006) Insulin secretory responses and phospholipid composition of pancreatic islets from mice that do not express group VIA phospholipase A_2 and effects of metabolic stress on glucose homeostasis. *J. Biol. Chem.* **281,** 20958–20973
27. Bao, S., Jacobson, D. A., Wohltmann, M., Bohrer, A., Jin, W., Philipson, L. H., and Turk, J. (2008) Glucose homeostasis, insulin secretion, and islet phospholipids in mice that overexpress iPLA$_2\beta$ in pancreatic β-cells and in iPLA$_2\beta$-null mice. *Am. J. Physiol. Endocrinol. Metab.* **294,** E217–E229
28. Pappan, K. L., Pan, Z., Kwon, G., Marshall, C. A., Coleman, T., Goldberg, I. J., McDaniel, M. L., and Semenkovich, C. F. (2005) Pancreatic β-cell lipoprotein lipase independently regulates islet glucose metabolism and normal insulin secretion. *J. Biol. Chem.* **280,** 9023–9029
29. Ma, Z., Bohrer, A., Wohltmann, M., Ramanadham, S., Hsu, F. F., and Turk, J. (2001) Studies of phospholipid metabolism, proliferation, and secretion of stably transfected insulinoma cells that overexpress group VIA phospholipase A_2. *Lipids* **36,** 689–700
30. Bao, S., Bohrer, A., Ramanadham, S., Jin, W., Zhang, S., and Turk, J. (2006) Effects of stable suppression of group VIA phospholipase A_2 expression on phospholipid content and composition, insulin secretion, and proliferation of INS-1 insulinoma cells. *J. Biol. Chem.* **281,** 187–198
31. Ren, Y. G., Wagner, K. W., Knee, D. A., Aza-Blanc, P., Nasoff, M., and Deveraux, Q. L. (2004) Differential regulation of the TRAIL death receptors DR4 and DR5 by the signal recognition particle. *Mol. Biol. Cell* **15,** 5064–5074
32. Hsu, F. F., Turk, J., Stewart, M. E., and Downing, D. T. (2002) Structural studies on ceramides as lithiated adducts by low energy collisional-activated dissociation tandem mass spectrometry with electrospray ionization. *J. Am. Soc. Mass Spectrom.* **13,** 680–695
33. Song, H., Bao, S., Ramanadham, S., and Turk, J. (2006) Effects of biological oxidants on the catalytic activity and structure of group VIA phospholipase A_2. *Biochemistry* **45,** 6392–6406
34. Bao, S., Jin, C., Zhang, S., Turk, J., Ma, Z., and Ramanadham, S. (2004) β-Cell calcium-independent group VIA phospholipase A_2 (iPLA$_2\beta$): tracking iPLA$_2\beta$ movements in response to stimulation with insulin secretagogues in INS-1 cells. *Diabetes* **53,** Suppl. 1, S186–S189
35. Song, H., Bao S., Lei, X., Jin, C., Zhang, S., Turk, J., and Ramanadham, S. (2010) Evidence for proteolytic processing and stimulated organelle redistribution of iPLA$_2\beta$. *Biochim. Biophys. Acta* **1801,** 547–558
36. Lei, X., Zhang, S., Bohrer, A., and Ramanadham, S. (2008) Calcium-independent phospholipase A_2 (iPLA$_2\beta$)-mediated ceramide generation plays a key role in the cross-talk between the endoplasmic reticulum (ER) and mitochondria during ER stress-induced insulin-secreting cell apoptosis. *J. Biol. Chem.* **283,** 34819–34832
37. Song, H., Rohrs, H., Tan, M., Wohltmann, M., Ladenson, J. H., and Turk, J. (2010) Effects of ER stress on group VIA PLA_2 (iPLA$_2\beta$) in β cells include tyrosine phosphorylation and increased association with calnexin. *J. Biol. Chem.* **285,** 33843–33857
38. Song, H., Hecimovic, S., Goate, A., Hsu, F. F., Bao, S., Vidavsky, I., Ramanadham, S., and Turk, J. (2004) Characterization of N-terminal processing of group VIA phospholipase A_2 and of potential cleavage sites of amyloid precursor protein constructs by automated identification of signature peptides in LC/MS/MS analyses of proteolytic digests. *J. Am. Soc. Mass Spectrom.* **15,** 1780–1793
39. Liu, W., Porter, N. A., Schneider, C., Brash, A. R., and Yin, H. (2011) Formation of 4-hydroxynonenal from cardiolipin oxidation: intramolecular peroxyl radical addition and decomposition. *Free Radic. Biol. Med.* **50,** 166–178
40. Hsu, F. F., Turk, J., Rhoades, E. R., Russell, D. G., Shi, Y., and Groisman, E. A. (2005) Structural characterization of cardiolipin by tandem quadrupole and multiple-stage quadrupole ion-trap mass spectrometry with electrospray ionization. *J. Am. Soc. Mass Spectrom.* **16,** 491–504
41. O'Donnell, V. B. (2011) Mass spectrometry analysis of oxidized phosphatidylcholine and phosphatidylethanolamine. *Biochim. Biophys. Acta* **1811,** 818–826
42. Hu, C., van Dommelen, J., van der Heijden, R., Spijksma, G., Reijmers, T. H., Wang, M., Slee, E., Lu, X., Xu, G., van der Greef, J., and Hankemeier, T. (2008) RPLC-ion-trap-FTMS method for lipid profiling of plasma: method validation and application to p53 mutant mouse model. *J. Proteome Res.* **7,** 4982–4991
43. Lakhani, S. A., Masud, A., Kuida, K., Porter, G. A. Jr., Booth, C. J., Mehal, W. Z., Inayat, I., and Flavell, R. A. (2006) Caspases 3 and 7: key mediators of mitochondrial events of apoptosis. *Science* **311,** 847–851
44. Ron, D. (2002) Translational control in the endoplasmic reticulum stress response. *J. Clin. Investig.* **110,** 1383–1388
45. Oyadomari, S., and Mori, M. (2004) Roles of CHOP/GADD153 in endoplasmic reticulum stress. *Cell Death Differ.* **11,** 381–389
46. Harding, H. P., Novoa, I., Zhang, Y., Zeng, H., Wek, R., Schapira, M., and Ron, D. (2000) Regulated translation initiation controls stress-induced gene expression in mammalian cells. *Mol. Cell* **6,** 1099–1108
47. Rutkowski, D. T., and Kaufman, R. J. (2004) A trip to the ER: coping with stress. *Trends Cell Biol.* **14,** 20–28
48. Ma, Y., Brewer, J. W., Diehl, J. A., and Hendershot, L. M. (2002) Two distinct stress signaling pathways converge upon the CHOP promoter during the mammalian un-folded protein response. *J. Mol. Biol.* **318,** 1351–1365
49. Piro, S., Anello, M., Di Pietro, C., Lizzio, M. N., Patanè, G., Rabuazzo, A. M., Vigneri, R., Purrello, M., and Purrello, F. (2002) Chronic exposure to free fatty acids or high glucose induces apoptosis in rat pancreatic islets: possible role of oxidative stress. *Metabolism* **51,** 1340–1347
50. Won, J. S., Im, Y. B., Khan, M., Singh, A. K., and Singh, I. (2004) The role of neutral sphingomyelinase produced ceramide in lipopolysaccharide-mediated expression of inducible nitric oxide synthase. *J. Neurochem.* **88,** 583–593
51. Zeng, C., Lee, J. T., Chen, H., Chen, S., Hsu, C. Y., and Xu, J. (2005) Amyloid-β peptide enhances tumor necrosis factor-α-induced iNOS through neutral sphingomyelinase/ceramide pathway in oligodendrocytes. *J. Neurochem.* **94,** 703–712
52. Veluthakal, R., Palanivel, R., Zhao, Y., McDonald, P., Gruber, S., and Kowluru, A. (2005) Ceramide induces mitochondrial abnormalities in insulin-secreting INS-1 cells: potential mechanisms underlying cer-

amide-mediated metabolic dysfunction of the β cell. *Apoptosis* **10,** 841–850

53. Gottlieb, E., Armour, S. M., Harris, M. H., and Thompson, C. B. (2003) Mitochondrial membrane potential regulates matrix configuration and cytochrome c release during apoptosis. *Cell Death Differ.* **10,** 709–717
54. Körper, S., Nolte, F., Rojewski, M. T., Thiel, E., and Schrezenmeier, H. (2003) The K^+ channel openers diazoxide and NS1619 induce depolarization of mitochondria and have differential effects on cell Ca^{2+} in CD34+ cell line KG-1a. *Exp. Hematol.* **31,** 815–823
55. Mancuso, D. J., Jenkins, C. M., Sims, H. F., Cohen, J. M., Yang, J., and Gross, R. W. (2004) Complex transcriptional and translational regulation of iPLA$_2\gamma$ resulting in multiple gene products containing dual competing sites for mitochondrial or peroxisomal localization. *Eur. J. Biochem.* **271,** 4709–4724
56. Ramanadham, S., Song, H., Bao, S., Hsu, F. F., Zhang, S., Ma, Z., Jin, C., and Turk, J. (2004) Islet complex lipid involvement in the actions of group VIA calcium-independent phospholipase A_2 in β cells. *Diabetes* **53,** Suppl. 1, S179–S185
57. Ramanadham, S., Song, H., Hsu, F. F., Zhang, S., Crankshaw, M., Grant, G. A., Newgard, C. B., Bao, S., Ma, Z., and Turk, J. (2003) Pancreatic islets and insulinoma cells express a novel isoform of group VIA phospholipase A_2 (iPLA$_2\beta$) that participates in glucose-stimulated insulin secretion and is not produced by alternate splicing of the iPLA$_2\beta$ transcript. *Biochemistry* **42,** 13929–13940
58. Michalska, M., Wolf, G., Walther, R., and Newsholme, P. (2010) Effects of pharmacological inhibition of NADPH oxidase or iNOS on pro-inflammatory cytokine, palmitic acid or H_2O_2-induced mouse islet or clonal pancreatic β-cell dysfunction. *Biosci. Rep.* **30,** 445–453
59. Listenberger, L. L., Ory, D. S., and Schaffer, J. E. (2001) Palmitate-induced apoptosis can occur through a ceramide-independent pathway. *J. Biol. Chem.* **276,** 14890–14895
60. Yuzefovych, L., Wilson, G., and Rachek, L. (2010) Different effects of oleate vs. palmitate on mitochondrial function, apoptosis, and insulin signaling in L6 skeletal muscle cells: role of oxidative stress. *Am. J. Physiol. Endocrinol. Metab.* **299,** E1096–E1105
61. Abaraviciene, S. M., Lundquist, I., and Salehi, A. (2008) Rosiglitazone counteracts palmitate-induced β-cell dysfunction by suppression of MAP kinase, inducible nitric oxide synthase and caspase 3 activities. *Cell. Mol. Life Sci.* **65,** 2256–2265
62. Keane, D. C., Takahashi, H. K., Dhayal, S., Morgan, N. G., Curi, R., and Newsholme, P. (2011) Arachidonic acid actions on functional integrity and attenuation of the negative effects of palmitic acid in a clonal pancreatic β-cell line. *Clin. Sci.* **120,** 195–206
63. Tsang, M. Y., Cowie, S. E., and Rabkin, S. W. (2004) Palmitate increases nitric oxide synthase activity that is involved in palmitate-induced cell death in cardiomyocytes. *Nitric Oxide* **10,** 11–19
64. Jeon, M. J., Leem, J., Ko, M. S., Jang, J. E., Park, H. S., Kim, H. S., Kim, M., Kim, E. H., Yoo, H. J., Lee, C. H., Park, I. S., Lee, K. U., and Koh, E. H. (2012) Mitochondrial dysfunction and activation of iNOS are responsible for the palmitate-induced decrease in adiponectin synthesis in 3T3L1 adipocytes. *Exp. Mol. Med.* **44,** 562–570
65. Ushmorov, A., Ratter, F., Lehmann, V., Dröge, W., Schirrmacher, V., and Umansky, V. (1999) Nitric oxide-induced apoptosis in human leukemic lines requires mitochondrial lipid degradation and cytochrome c release. *Blood* **93,** 2342–2352
66. Borutaite, V., and Brown, G. C. (2003) Nitric oxide induces apoptosis via hydrogen peroxide but necrosis via energy and thiol depletion. *Free Radic. Biol. Med.* **35,** 1457–1468
67. Montero, J., Mari, M., Colell, A., Morales, A., Basañez, G., Garcia-Ruiz, C., and Fernández-Checa, J. C. (2010) Cholesterol and peroxidized cardiolipin in mitochondrial membrane properties, permeabilization and cell death. *Biochim. Biophys. Acta* **1797,** 1217–1224
68. Balazy, M., and Nigam, S. (2003) Aging, lipid modifications and phospholipases—new concepts. *Ageing Res. Rev.* **2,** 191–209
69. McMillin, J. B., and Dowhan, W. (2002) Cardiolipin and apoptosis. *Biochim. Biophys. Acta* **1585,** 97–107
70. Malhotra, A., Edelman-Novemsky, I., Xu, Y., Plesken, H., Ma, J., Schlame, M., and Ren, M. (2009) Role of calcium-independent phospholipase A_2 in the pathogenesis of Barth syndrome. *Proc. Natl. Acad. Sci. U.S.A.* **106,** 2337–2341
71. Sparagna, G. C., and Lesnefsky, E. J. (2009) Cardiolipin remodeling in the heart. *J. Cardiovasc. Pharmacol.* **53,** 290–301
72. Zachman, D. K., Chicco, A. J., McCune, S. A., Murphy, R. C., Moore, R. L., and Sparagna, G. C. (2010) The role of calcium-independent phospholipase A_2 in cardiolipin remodeling in the spontaneously hypertensive heart failure rat heart. *J. Lipid Res.* **51,** 525–534
73. Ma, Z. A., Zhao, Z., and Turk, J. (2012) Mitochondrial dysfunction and β-cell failure in type 2 diabetes mellitus. *Exp. Diabetes Res.* **2012,** 703538
74. Ma, Z. A. (2012) The role of peroxidation of mitochondrial membrane phospholipids in pancreatic β-cell failure. *Curr. Diabetes Rev.* **8,** 69–75
75. Andersen, A. D., Poulsen, K. A., Lambert, I. H., and Pedersen, S. F. (2009) HL-1 mouse cardiomyocyte injury and death after simulated ischemia and reperfusion: roles of pH, Ca^{2+}-independent phospholipase A_2, and Na^+/H^+ exchange. *Am. J. Physiol. Cell Physiol.* **296,** C1227–C1242
76. Ramanadham, S., Hsu, F. F., Bohrer, A., Nowatzke, W., Ma, Z., and Turk, J. (1998) Electrospray ionization mass spectrometric analyses of phospholipids from rat and human pancreatic islets and subcellular membranes: comparison to other tissues and implications for membrane fusion in insulin exocytosis. *Biochemistry* **37,** 4553–4567
77. Wang, X., Li, H., De Leo, D., Guo, W., Koshkin, V., Fantus, I. G., Giacca, A., Chan, C. B., Der, S., and Wheeler, M. B. (2004) Gene and protein kinase expression profiling of reactive oxygen species-associated lipotoxicity in the pancreatic β-cell line MIN6. *Diabetes* **53,** 129–140
78. Wiederkehr, A., and Wollheim, C. B. (2009) Linking fatty acid stress to β-cell mitochondrial dynamics. *Diabetes* **58,** 2185–2186
79. Molina, A. J., Wikstrom, J. D., Stiles, L., Las G, Mohamed, H., Elorza, A., Walzer, G., Twig, G., Katz, S., Corkey, B. E., and Shirihai, O. S. (2009) Mitochondrial networking protects β-cells from nutrient-induced apoptosis. *Diabetes* **58,** 2303–2315
80. Vik, S. B., and Capaldi, R. A. (1977) Lipid requirements for cytochrome c oxidase activity. *Biochemistry* **16,** 5755–5759
81. Robinson, N. C., Strey, F., and Talbert, L. (1980) Investigation of the essential boundary layer phospholipids of cytochrome c oxidase using Triton X-100 delipidation. *Biochemistry* **19,** 3656–3661
82. Abramovitch, D. A., Marsh, D., and Powell, G. L. (1990) Activation of beef-heart cytochrome c oxidase by cardiolipin and analogues of cardiolipin. *Biochim. Biophys. Acta* **1020,** 34–42
83. Paradies, G., Ruggiero, F. M., Dinoi, P., Petrosillo, G., and Quagliariello, E. (1993) Decreased cytochrome oxidase activity and changes in phospholipids in heart mitochondria from hypothyroid rats. *Arch. Biochem. Biophys.* **307,** 91–95
84. Ott, M., Robertson, J. D., Gogvadze, V., Zhivotovsky, B., and Orrenius, S. (2002) Cytochrome c release from mitochondria proceeds by a two-step process. *Proc. Natl. Acad. Sci. U.S.A.* **99,** 1259–1263
85. Spooner, P. J., and Watts, A. (1992) Cytochrome c interactions with cardiolipin in bilayers: a multinuclear magic-angle spinning NMR study. *Biochemistry* **31,** 10129–10138
86. Salamon, Z., and Tollin, G. (1997) Interaction of horse heart cytochrome c with lipid bilayer membranes: effects on redox potentials. *J. Bioenerg. Biomembr.* **29,** 211–221
87. Shidoji, Y., Hayashi, K., Komura, S., Ohishi, N., and Yagi, K. (1999) Loss of molecular interaction between cytochrome c and cardiolipin due to lipid peroxidation. *Biochem. Biophys. Res. Commun.* **264,** 343–347
88. Rytömaa, M., and Kinnunen, P. K. (1994) Evidence for two distinct acidic phospholipid-binding sites in cytochrome *c. J. Biol. Chem.* **269,** 1770–1774
89. Williams, S. D., and Gottlieb, R. A. (2002) Inhibition of mitochondrial calcium-independent phospholipase A_2 (iPLA$_2$) attenuates mitochondrial phospholipid loss and is cardioprotective. *Biochem. J.* **362,** 23–32
90. Gadd, M. E., Broekemeier, K. M., Crouser, E. D., Kumar, J., Graff, G., and Pfeiffer, D. R. (2006) Mitochondrial iPLA$_2$ activity modulates the release of cytochrome *c* from mitochondria and influences the permeability transition. *J. Biol. Chem.* **281,** 6931–6939
91. Xu, Y., Malhotra, A., Ren, M., and Schlame, M. (2006) The enzymatic function of tafazzin. *J. Biol. Chem.* **281,** 39217–39224
92. Ma, B. J., Taylor, W. A., Dolinsky, V. W., and Hatch, G. M. (1999) Acy-

lation of monolysocardiolipin in rat heart. *J. Lipid Res.* **40,** 1837–1845
93. van Kuijk, F. J., Sevanian, A., Handelman, G. J., and Dratz, E. A. (1987) A new role for phospholipase A_2: protection of membranes from lipid peroxidation damage. *Trends Biochem. Sci.* **12,** 31–34
94. Kinsey, G. R., Blum, J. L., Covington, M. D., Cummings, B. S., McHowat, J., and Schnellmann, R. G. (2008) Decreased iPLA$_2\gamma$ expression induces lipid peroxidation and cell death and sensitizes cells to oxidant-induced apoptosis. *J. Lipid Res.* **49,** 1477–1487
95. Cummings, B. S., McHowat, J., and Schnellmann, R. G. (2002) Role of an endoplasmic reticulum Ca^{2+}-independent phospholipase A_2 in oxidant-induced renal cell death. *Am. J. Physiol. Renal Physiol.* **283,** F492–F498
96. Kinsey, G. R., McHowat, J., Beckett, C. S., and Schnellmann, R. G. (2007) Identification of calcium-independent phospholipase $A_2\gamma$ in mitochondria and its role in mitochondrial oxidative stress. *Am. J. Physiol. Renal Physiol.* **292,** F853–F860
97. Hazen, S. L., Zupan, L. A., Weiss, R. H., Getman, D. P., and Gross, R. W. (1991) Suicide inhibition of canine myocardial cytosolic calcium-independent phospholipase A_2. Mechanism-based discrimination between calcium-dependent and -independent phospholipases A_2. *J. Biol. Chem.* **266,** 7227–7232
98. Zupan, L. A., Weiss, R. H., Hazen, S. L., Parnas, B. L., Aston, K. W., Lennon, P. J., Getman, D. P., and Gross, R. W. (1993) Structural determinants of haloenol lactone-mediated suicide inhibition of canine myocardial calcium-independent phospholipase A_2. *J. Med. Chem.* **36,** 95–100
99. Balsinde, J., Bianco, I. D., Ackermann, E. J., Conde-Frieboes, K., and Dennis, E. A. (1995) Inhibition of calcium-independent phospholipase A_2 prevents arachidonic acid incorporation and phospholipid remodeling in P388D1 macrophages. *Proc. Natl. Acad. Sci. U.S.A.* **92,** 8527–8531
100. Balsinde, J., Balboa M. A., and Dennis, E. A. (1997) Antisense inhibition of group VI Ca^{2+}-independent phospholipase A_2 blocks phospholipid fatty acid remodeling in murine P388D1 macrophages. *J. Biol. Chem.* **272,** 29317–29321
101. Six, D. A., and Dennis, E. A. (2000) The expanding superfamily of phospholipase A_2 enzymes: classification and characterization. *Biochim. Biophys. Acta* **1488,** 1–19
102. Balsinde, J., and Balboa, M. A. (2005) Cellular regulation and proposed biological functions of group VIA calcium-independent phospholipase A_2 in activated cells. *Cell. Signal.* **17,** 1052–1062
103. Martínez, J., and Moreno, J. J. (2001) Role of Ca^{2+}-independent phospholipase A_2 on arachidonic acid release induced by reactive oxygen species. *Arch. Biochem. Biophys.* **392,** 257–262
104. Pérez, R., Melero, R., Balboa, M. A., and Balsinde, J. (2004) Role of group VIA calcium-independent phospholipase A_2 in arachidonic acid release, phospholipid fatty acid incorporation, and apoptosis in U937 cells responding to hydrogen peroxide. *J. Biol. Chem.* **279,** 40385–40391
105. Balboa, M. A., and Balsinde, J. (2006) Oxidative stress and arachidonic acid mobilization. *Biochim. Biophys. Acta* **1761,** 385–391
106. Tang, J., Kriz, R. W., Wolfman, N., Shaffer, M., Seehra, J., and Jones, S. S. (1997) A novel cytosolic calcium-independent phospholipase A_2 contains eight ankyrin motifs. *J. Biol. Chem.* **272,** 8567–8575
107. Chen, X., Zhang, W., Laird, J., Hazen, S. L., and Salomon, R. G. (2008) Polyunsaturated phospholipids promote the oxidation and fragmentation of γ-hydroxyalkenals: formation and reactions of oxidatively truncated ether phospholipids. *J. Lipid Res.* **49,** 832–846
108. Burke, J. E., and Dennis, E. A. (2009) Phospholipase A_2 structure/function, mechanism, and signaling. *J. Lipid Res.* **50,** (Suppl.) S237–S242
109. Nigam, S., and Schewe, T. (2000) Phospholipase A_2s and lipid peroxidation. *Biochim. Biophys. Acta* **1488,** 167–181
110. Yang, W. Y., Zheng, Y., Bahn, S. C., Pan, X. Q., Li, M. Y., Vu, H. S., Roth, M. R., Scheu, B., Welti, R., Hong, Y. Y., and Wang, X. M. (2012) The patatin-containing phospholipase A pPLAIIα modulates oxylipin formation and water loss in *Arabidopsis thaliana*. *Mol. Plant* **5,** 452–460